



# Cooling Load Prediction in Residential Buildings via a Two-Phase Whale Optimization Algorithm

Gurpreet Singh Sokhal<sup>1</sup>, Gurprinder Singh Dhindsa<sup>1</sup>, Rupinder Singh<sup>1</sup>, Narinder Singh<sup>1</sup>, Jugraj Singh Randhawa<sup>2</sup>

1. Department of Mechanical Engineering, Chandigarh University, Gharuan, Punjab, India – 140413

2. Khalsa College of Engineering & Technology, Amritsar, Punjab, India, - 143001

## Article Info

Received 1 June 2025

Received in Revised form 16 July 2025

Accepted 18 July 2025

Published online 21 July 2025

DOI: <https://doi.org/10.5185/aisesj.2025.1.1.37-60>

## Keywords

Residential buildings

Computational Intelligence

WOA

Hybrid

## Abstract

Evaluating the energy efficiency of energy-efficient constructions relies heavily on accurately anticipating their thermal loads. Current results have demonstrated that stochastic algorithms effectively tackle the abovementioned problem. In light of these issues, this research aims to evaluate a novel hybrid technique for estimating dwellings' cooling load (CL). The multilayer perceptron and the Whale Optimization Algorithm (WOA-MLP) are both suggested components of the model. The nonlinear analysis of the impact of eight freestanding parameters on the cooling load was performed through the best structure of every model. The assessment for this investigation was carried out in two stages. During the first stage, the population size that yielded the highest coefficient of determination ( $R^2$ ) value and the lowest root mean square error (RMSE) amount was selected as the optimal one. During the second stage, the experiment's findings with a swarm size of 500 ( $R^2 = 0.95155$  and  $0.95021$ ,  $RMSE = 0.07973$  and  $0.07737$  for training and validation, correspondingly) were put through a series of tests using several various p values (between 0.5-1.4). According to the findings, the p-value of 1.3 is the one that provides the most reliable results. This amount has an  $R^2$  equal to 0.95212 and 0.94792 and an RMSE equal to 0.07926 and 0.07909.

## 1. Introduction

Construction, transportation, and industrial production are the three most significant energy consumers worldwide [1-3]. Buildings are expected to account for over a third of total consumption by 2040 [4]. Energy-efficient constructions have been proposed to meet the growing preference for smart cities[5, 6]. This goal may be significantly advanced by accurately assessing a building's energy performance (EPB). Cooling load (CL) and heating load (HL) and requirements contribute to energy-efficient buildings' overall energy consumption. These loads are managed by a heating, ventilation, and air conditioning (HVAC) system [7] so as to ensure that the building's occupants are comfortable in the interior environment. People's daily lives are significantly impacted by both price and energy consumption. As a result, coupled with environmental problems,

various difficulties like acid rain, dependence on diminishing fossil fuel sources, emissions of greenhouse gas [8-16], and change of climate [17-20] develop due to the amount of energy used in conjunction with the availability of energy [2, 21, 22]. In recent years, many strategies have been utilized to design the HVAC system most efficiently [23-31]. For example, Ghahramani et al. [32] employed a systematic approach to improving skyscrapers' HVAC operation concerning the operating temperature point. In addition to that, Ferreira et al. [33] controlled the HVAC system by using an approach that employed soft computing. When the suggested approach was implemented, it reduced energy use by around fifty percent.

In this manner, some of the limitations of conventional current modeling methodologies (for example, simulation packages of modeling), like



Corresponding author: [rupinder\\_singh302@yahoo.com](mailto:rupinder_singh302@yahoo.com) (Rupinder Singh)

inadequacies and enormous dimensions for crowded places [34], have prompted engineers to utilize AI (artificial intelligence) technologies for quick prediction of energy [35, 36]. The term "artificial intelligence" refers to the problem-solving abilities shown by computers and other electronic devices, in contrast to the "natural intelligence" displayed by living things such as people and animals [37-41]. As probably one of the best AI-based alternatives, artificial neural networks, or ANNs, have lately garnered increasing interest [42-45]. In principle, the theories established upon deep learning [46-48], machine learning [49, 50], decision-making, the alternatives which are based on feature selection [51, 52], extremer machine learning [53-55], and hybrid algorithms increasing conventional multilayer perceptron. These methods are effective in a variety of contexts, including the design of buildings [56-63], the analysis and categorization of images [63-69], durability, and environmental issues [70-72]. In addition, various research has been done to forecast the HL and CL in green buildings [73-75]. To precisely estimate the thermal load in a scholarly building, Zhou et al. [31] utilized an ANN in conjunction with the nonlinear autoregressive with exogenous inputs (NARX) paradigm. Comparative research was carried out by Koschwitz et al. [76], who used NARX recurrent neural networks (NARX RNNs) to approximate longstanding metropolitan heating loads. Neural networks performed far superior to other traditional approaches like gradient-boosted machines, according to research published by Roy et al. [77], which indicated that neural networks accounted for 99.76 percent of the variation in the data.

Various forecasters, like adaptive neuro-fuzzy inference systems (ANFISs), have demonstrated excellent resilience when handling nonlinear issues [78]. Pezeshki and Mazinani [79] deduced that ANFISs are more remarkable than traditional fuzzy logic regarding the thermal performance of green buildings. This is because ANFISs also delight in all of the benefits that ANNs do. The practical application of support vector-based approaches and ANFIS has been illustrated by researchers named Naji et al. [80] and Chou and Bui [81]. In more new findings, researchers have proposed combining traditionally used predictors with metaheuristic search strategies for various applications [82]. Even more dramatically, using these methods has significantly enhanced the reputation of energy consumption modeling. Satrio et al. demonstrated the effectiveness of

integrating ANNs and multiobjective genetic algorithms in improving HVAC systems, providing an efficient solution [83]. To forecast the amount of energy used by buildings, Moayedi et al. [4] combined an artificial neural network with an electromagnetism-based firefly algorithm. The research findings show the superiority of the proposed new model over traditional models. TienBui et al. [30] found that implementing the imperialist competition and genetic algorithms could decrease the ANN's HL forecast error from 2.93 to 2.06 and 2.00 in that order. This error decreased from 3.28 to 2.09 and then 2.10 for the CL measurement. In addition, research conducted by Nguyen et al. [84] and Moayedi et al. [85] utilized innovative metaheuristic strategies to improve the ANN's power to make accurate predictions. Despite the widespread application of nature-inspired metaheuristic tools to improve the HVAC system, the writers were motivated to examine the potential application of an innovative representative of this group, specifically stochastic fractal search, in this article due to the extensive diversity of these approaches. According to our knowledge, the aforementioned algorithm has never been utilized in this particular domain before.

This paper introduces a two-phase multiobjective optimization algorithm, the WOA, which extends a recent nature-inspired optimization algorithm to handle multiple objectives [86]. Previous research has attempted to solve multiobjective issues utilizing the WOA algorithm, including the non-dominated sorting based on the multiobjective Whale Optimization Algorithm (NSMOWOA) [87], which uses a new non-dominated sorting approach to evaluate the non-dominated solutions. Another approach proposed an external archive to store the nondominated solutions and employed a roulette wheel approach to modify the solutions' distribution in the archive [88]. Another method, Multiobjective WOA (MOWOA), incorporated archive grid selection in the original WOA [89]. In contrast, the proposed GPAWOA algorithm utilizes a simple and effective strategy to upgrade the external archive, which is crucial for the algorithm's convergence. It incorporates the crowding distance computation's mechanism at different algorithm steps to ensure well-distributed solutions in the archive. The WOA algorithm is easy to implement because of its simple mechanism, and the suggested WOA algorithm effectively balances exploitation and exploration of the search space and has high

convergence and success as a single-objective optimizer. This article is organized as: Section 2 describes the created database. The WOA and ANN are also briefly reviewed in Section 3. Section 4 represents experimental findings, comparisons, and test and performance measures. The article is finally concluded in Section 5, which covers future research.

## 2. Established database:

It is common knowledge that the correct construction of intelligent models requires the application of data that can be relied upon. In the context of this investigation, the data from a green building is taken into consideration. The dataset is generated through computer simulations conducted in the Ecotect environment [90]. Tsanas and Xifara [91] were the ones who came up with the idea, and you can find it at the mentioned URL:

<http://archive.ics.uci.edu/ml/datasets/Energy+efficiency>.

Through the examination of 12 distinct structures (a volume of 771.75 m<sup>3</sup>), the CL and HL [92] of 768 cases were gathered once relative compactness (RC) =  $\frac{6V^{\frac{2}{3}}}{A}$ , which denotes the ratio between the surface area (A) and the equivalent volume (V) [93]), overall height (OH), surface area (SA), wall area (WA), glazing area (GA), roof area (RA) [92, 94], orientation, which stands for the total area calculated by the rough opening, containing sash, glass, and frame [95], and the glazing area distribution (GAD), which stands for how the GA is spread out in the whole building [92], are considered essential parameters (that is, freestanding parameters). Figures 1 and 2 indicate the data preparation's graphical and schematic view.

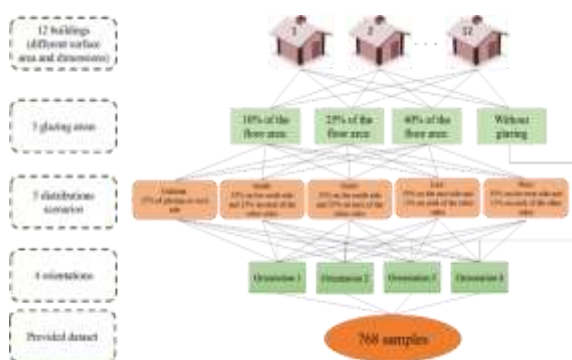
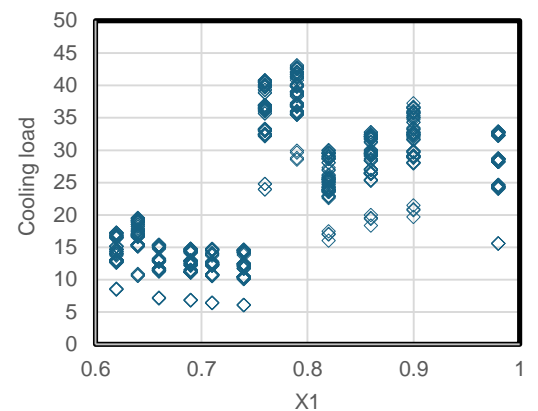
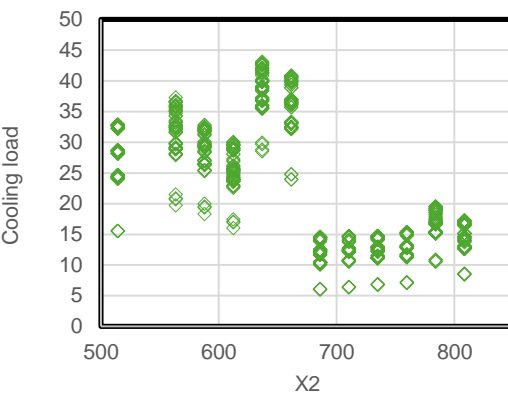


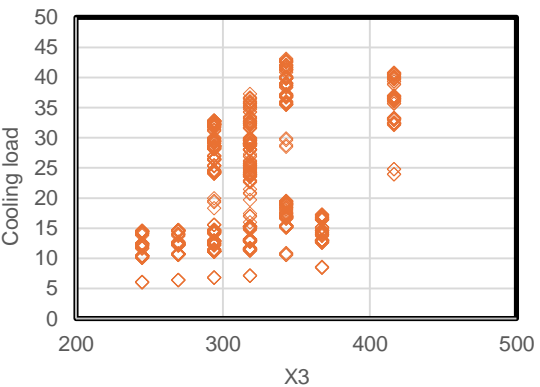
Figure 1. Preparation of data in a graphical view



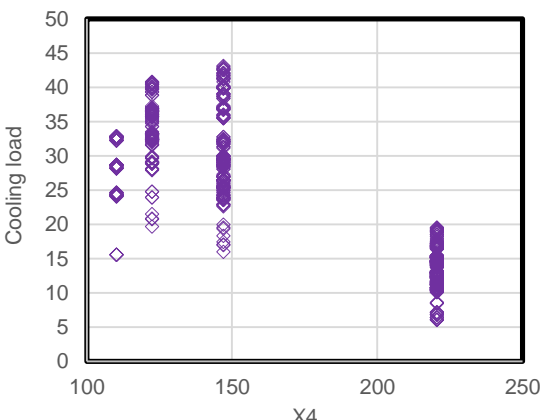
a) relative compactness (RC)



b) surface area



c) wall area



d) roof area

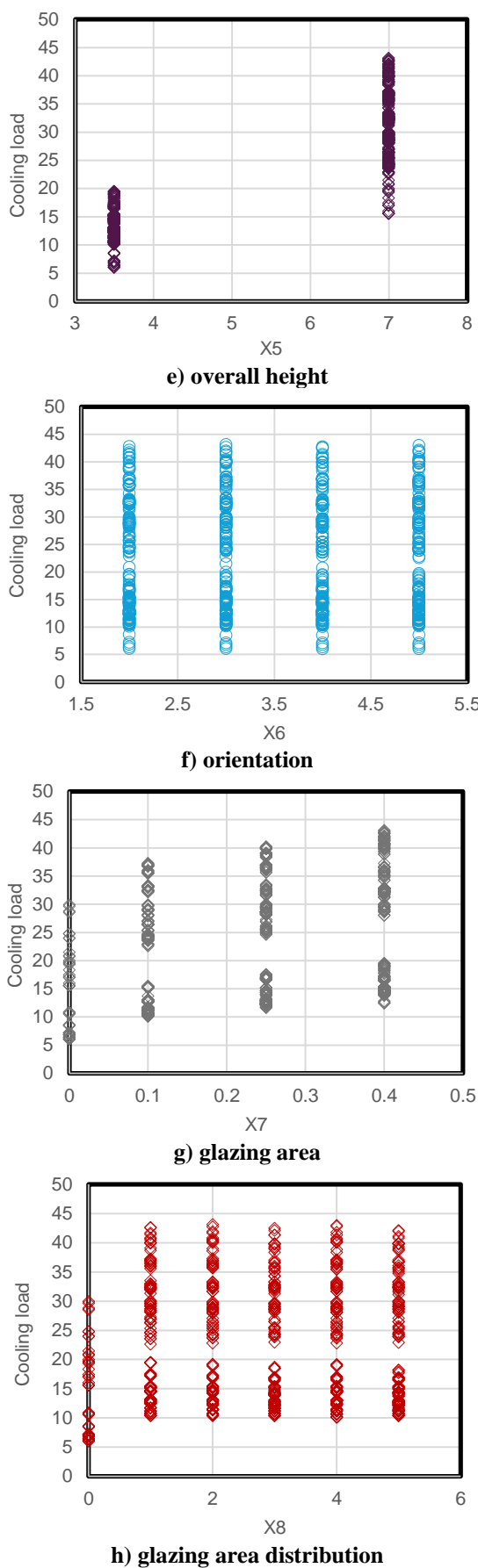


**Figure 2. Preparation of data in a schematic view versus cooling load**

Figure 3 shows the variable range for all eight input variables. Regarding this figure, overall height has the highest range, and wall area has the lowest range. Figures 4 and 5 demonstrate the variation of input parameters versus each other. The target amounts (cooling load) are divided into class I, II, and III grips. Class I is related to 12.38-23.3, class II ranges between 23.3-35.66, and the third-class ranges between 35.67- 48.04. Figure 5 demonstrates the variation of each of the two parameters versus each other.

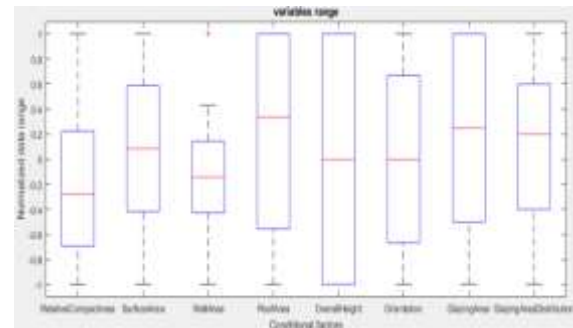


**Figure 3: The variables' range of input parameters**

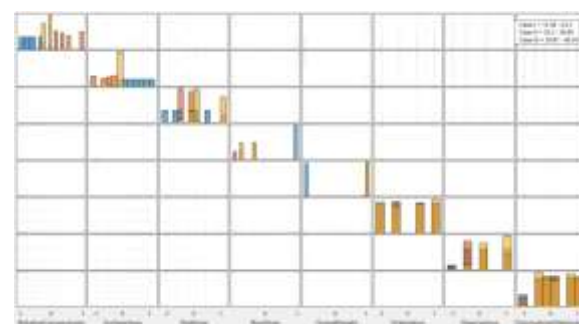
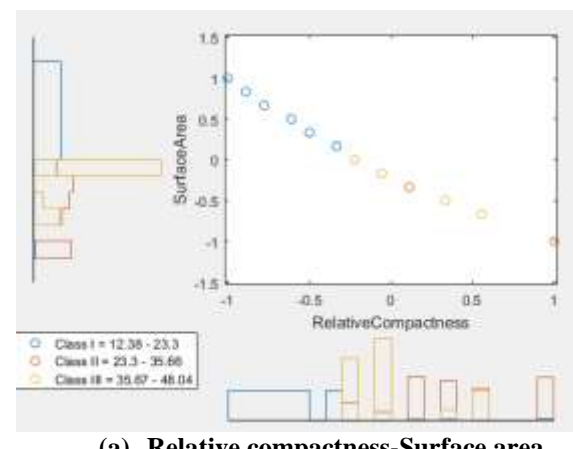


**Figure 4: Variation of input parameters**



**(a) Relative compactness-Surface area**

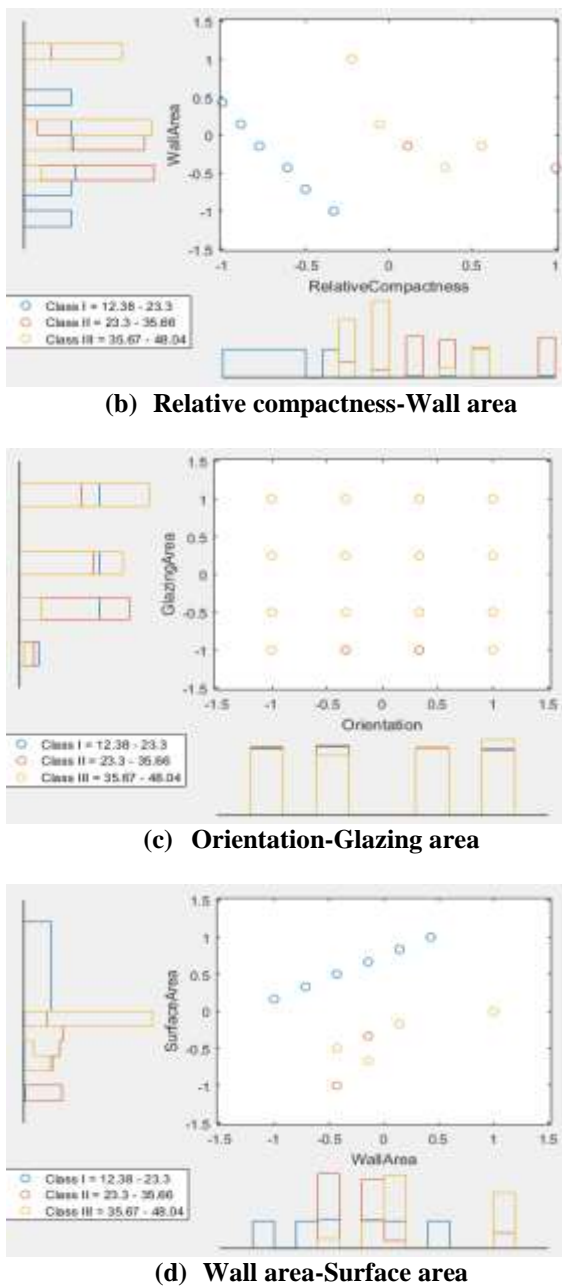


Figure 5: Variation of input parameters

Figure 6 presents the Andrews plot for our dataset. Andrews's plots, also known as Andrew's curves, were first introduced by George Andrews in 1972. They are a less well-known visualization technique but valuable in specific scenarios, such as when comparing multiple data sets with many variables. The basic idea behind Andrew's plot is to convert data points into curves. This is done by computing the Fourier series of the data, which decomposes it into a series of sine and cosine functions. The Fourier coefficients are then used to calculate and plot curve shapes. The resulting plot consists of multiple curves (one for each data point) overlaid on the same graph (Figure 6). Each

curve is represented in a different color, and labels can be added to clearly distinguish them from one another.

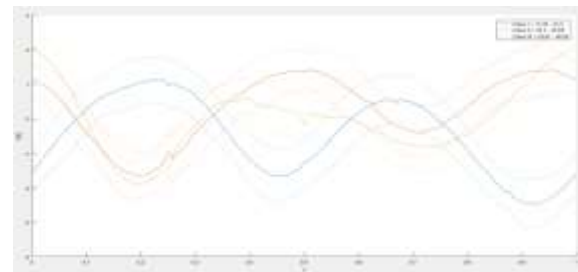


Figure 6: The description of Andrews plot for the input and output layers

### 3. Methodology

#### 3.1. Multilayer perceptron

In 1943, Pitts and McCulloch originally proposed an ANN's concept [96]. Scholars have recommended a diversity of ANNs for various applications because of their ability to map variables nonlinearly [97, 98]. There are several advantages to using the Multilayer Perceptron (MLP) tool over other ANN kinds, including its adaptability in terms of structure and its capacity to express a wide variety of data items. Backpropagation is the training method used for MLPs, also known as feedforward neural implements and generic approximators [99]. Neurons, a computing entity, can anticipate almost any input-output arrangement. This work shows MLPs in Fig. 7 as a schematic representation of their overall structure. As one can see, it comprises three unique levels: input and output layers and a hidden layer. A significant connection exists between the neurons in this layer(s) and those in the one above it [100, 101].

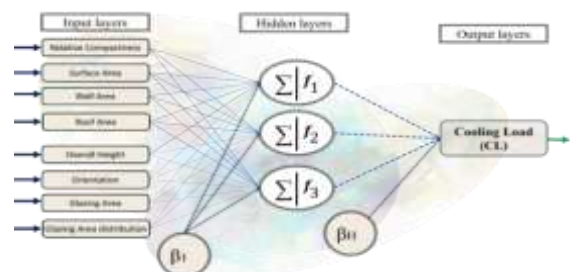


Figure 7: The general structure of the MLP

#### 3.2. Whale Optimization Algorithm (WOA):

In this part of the article, we will first go through the sources that inspired the technique offered. Afterward, the mathematical model is supplied.

### 3.2.1. Inspiration

Whales are perhaps of nature's most beautiful animals. There is no doubt that they are the most enormous land creatures on Earth. Mature whales may weigh up to 180 tons and 30 meters in length. Killer, minke, Sei, humpback, finback, right, and blue whales are among the seven major kinds of this enormous animal. They are often believed to be predatory. They cannot rest since they must get their air from the ocean's surface. In reality, just half of the brain rests throughout the night. What's fascinating about whales is that they're thought of as emotionally complex, highly cognitive creatures.

It has been suggested by Van Der Gucht and Hof [102] that whales have a kind of brain cell designated as spindle cells identical to humans. Neurons in the brain's limbic system are essential for human judgment, emotional responses, and social interaction. We are unique from other animals because of the spindle cells. Because whales have double the amount of these cells as an adult person, they are brilliant. Whales are capable of learning, thinking, communicating, judging, and being emotional, although clearly at a lesser level of intelligence than humans. Whales (especially killer whales) have been reported to be capable of developing their dialects. It is also fascinating to see how whales interact with each other socially. They may either be found living alone or in small groups. The majority of the time, however, they are found in packs. Some animals (such as killer whales) may remain together as a colony for the whole of their lives. Huge humpbacks (*Megaptera novaeangliae*) are a large species of baleen whale. Adult humpback whales are around a school bus's size when fully grown. Krill and groups of juvenile fish are their preferred food source. In Fig. 8, you can see this creature in action.

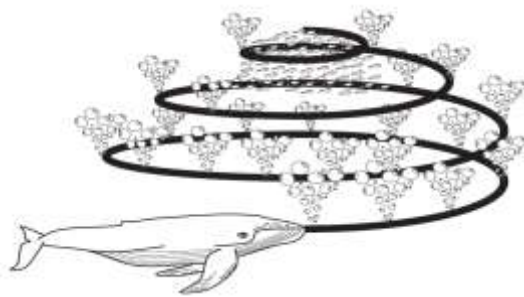


**Figure 8: Bubble-net feeding humpback whales' behavior.**

The unique hunting style of humpback whales' is perhaps the most fascinating aspect of these animals. The form of feeding known as bubble-net feeding refers to this kind of foraging activity [103]. Humpback whales must stay near the surface to catch tiny fish or krill. Figure 8 shows this foraging by forming different bubbles across a circular or '9'-shaped route. Before 2011, this phenomenon was solely researched on the basis of observations made from the surface.

On the other hand, Goldbogen et al. [104] utilized tag sensors to study this behavior. They recorded 300 bubble-net feeding occurrences of nine unique humpback whales, all tracked by tags. 'Upward spirals' and 'double-loops' were the two techniques they discovered connected with bubbles. In the first technique, they descend to around 12 meters below the surface, constructing a spiraling bubble around their prey before swimming back up to the top. The latter move includes three distinct steps: the catch loop, the lobtail, and the coral loop. This behavior's specifics may be discovered in [104]. It is essential to note that humpback whales are the only marine mammals known to engage in the unusual eating method known as bubble-net feeding. Within the scope of this study, a theoretical formalism of the spiral bubble-net feeding method is constructed to facilitate optimization.

### 3.2.2. Optimization Algorithm and Mathematical Model

The first thing presented in this chapter is encircling prey's mathematical model, followed by a spiral bubble-net feeding strategy and a hunt for food. The WOA algorithm is then put out as a solution to this issue.

### 3.2.3. Encircling prey

The humpback whale can locate and encircle prey that it recognizes. Because the precise location of the finest potential solution in the search zone cannot be determined in advance, the WOA approach assumes that the best available candidate solution is either the target prey or is very near to the ideal solution. As soon as the leading search agent has been identified, the other search agents will work to improve their standings concerning the top search agent. The following equations provide a representation of this pattern of behavior:

$$\vec{D} = |\vec{C} * \vec{X}^*(t) - \vec{X}(t)| \quad (1)$$

$$\vec{X}(t+1) = \vec{X}^*(t) - \vec{A} \cdot \vec{D} \quad (2)$$

In this equation,  $t$  stands for the current repetition,  $\vec{C}$  and  $\vec{A}$  are vectors of coefficient, and  $X^*$  is a vector of position representing the most excellent solution found thus far. In addition,  $X$  is a situation vector representing the worst solution found thus far. The notation  $||$  denotes the absolute value, whereas the symbol  $\cdot$  denotes the element-by-element multiplication. It is essential to point out that if there is a better answer,  $X^*$  should be modified after each repetition of the problem-solving process.

The vectors  $\vec{C}$  and  $\vec{A}$  are determined utilizing the following formulas:

$$\vec{A} = 2\vec{a} \cdot \vec{r} - \vec{a} \quad (3)$$

$$\vec{C} = 2 \cdot \vec{r} \quad (4)$$

Where  $\vec{a}$  is an accidental vector and is changed linearly from 0 to 2 throughout iterations (in both the exploration and exploitation stages), and where  $\vec{r}$  is a vector in the  $[0, 1]$  range.

To further understand the underlying reasoning of Eq. (2), consider the 2D situation shown in Fig. 9. It is possible to adjust a search agent's position ( $X, Y$ ) such that it corresponds with the location of the record that is now considered to be the best ( $X^*, Y^*$ ).

By modifying the value of  $\vec{C}$  and  $\vec{A}$  vectors, it is possible to move to various locations about the present position and remain near the best agent. In addition, the potential updated location of a search agent in three-dimensional space is represented in Fig. 9 (b). As illustrated in Figure 9, it is feasible to go anywhere in the search space between the critical locations by specifying an appropriate random vector ( $\vec{r}$ ). Equation (2.2) enables any search agent to imitate encircling the prey by constantly updating its location near the most outstanding solution.

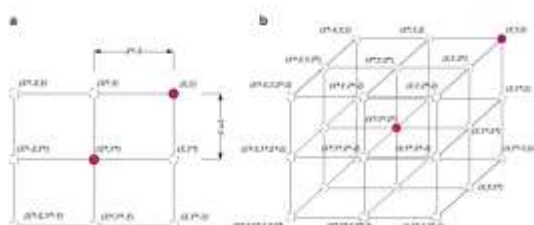


**Figure 9: 3D and 2D position vectors and their feasible following locations**

The identical notion may be generalized to a space of search with  $n$  dimensions; in which case the search agents will travel in hyper-cubes of the most excellent solution achieved up to this point. As was covered in the prior part of this article, humpback whales are also known to hunt their prey using the bubble-net method. Quantitatively, the following is how this approach is put together:

### 3.2.3.1. Bubble-net attacking method (exploitation phase)

To simulate the humpback whales' bubble-net treatment, two following methods are designed: Two methods, which are described in the following sequence, have been devised to mimic the humpback whales' bubble-net behavior quantitatively:

**1. Shrinking encircling mechanism:**  $\vec{a}$  in the equation may be made to behave in this manner by lowering the value it has in Eq. (2.3). It is worth noting that  $\vec{A}$ 's fluctuation range has shrunk by  $\vec{a}$ . To put it another way,  $\vec{A}$  is a number that is chosen at random from the range  $[-a, a]$ , where  $a$  is dropped from 2 to 0 as the iteration process continues. By assigning random values to  $\vec{A}$  in the range of  $[-1, 1]$ , the new location of a search agent may be determined anywhere in the range between the agent's starting position and the situation of the most excellent agent currently available. The feasible locations from  $(X, Y)$  approaching  $(X^*, Y^*)$  that can be obtained by  $0 \leq A \leq 1$  in a two-dimensional space are shown in Fig. 10a.

**2. Spiral updating position:** This method begins by computing the distance between the whale, which is positioned at the coordinates  $(X, Y)$ , and the prey, which is placed at the coordinates  $(X^*, Y^*)$ , as shown in Fig. 10 (b). After that, a spiral equation is built between the location of the prey and the whale to model the helix-shaped motion that humpback whales make, and it looks like this:

$$X^*(t+1) = e^{bl} \cdot \cos(2\pi k) \cdot (D^*)^* + (X^*)^*(t) \quad (5)$$

where  $\vec{D}^* = |\vec{X}^*(t) - \vec{X}(t)|$  is the distance between the prey and the  $i$ th whale (the most excellent solution found thus far),  $b$  is a constant that represents the logarithmic spiral's shape,  $l$  is an accidental integer in the range of  $[-1, 1]$ .

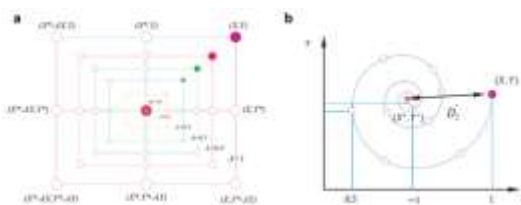


**Figure 10: The WOA algorithm's Bubble-net's search mechanism: (a) the mechanism of shrinking encircling and (b) the position of spiral updating.**

It is essential to know that humpback whales method their prey in a contracting circle while concurrently following a spiraling course. For the sake of modeling this concurrent behavior, we postulate that there is a chance of fifty percent to select either the shrinking encircling mechanism or the spiral method to adjust the location of whales while optimization is in progress. The following is a description of the mathematical model:

$$\vec{X}(t+1) = \begin{cases} \vec{X}^*(t) - \vec{A} \cdot \vec{D} & \text{if } p < 0.5 \\ e^{bt} \cdot \cos(2\pi k) \cdot \vec{D}' + \vec{X}^*(t) & \text{if } p \geq 0.5 \end{cases} \quad (6)$$

In which  $p$  is an accidental integer that falls between 0 and 1.

The humpback whales will randomly seek food and use the bubble-net approach. The following subsection is a mathematical method of how the search is being carried out.

### 3.2.3.2. Search for prey (exploration stage)

Searching for prey may also make use of  $\vec{A}$  vector variant and the corresponding strategy (examination). Admittedly, humpback whales look about haphazardly, taking into account where each other is located. As a result, we utilize  $\vec{A}$  with random values that are either more than one or less than -1 to coerce the search agent to go a significant space away from a reference whale. In the exploration stage, we do not use the most outstanding search agent we have discovered thus far to change the situation of a search agent. Instead, we choose a search agent at random. This technique, together with  $|\vec{A}| > 1$ , emphasizes exploration and makes it possible for the WOA method to conduct a worldwide search. Following are some of the details of the mathematical model:

$$\vec{P} \equiv |\vec{C} \cdot \overrightarrow{X_{rcmd}} - \vec{X}(t)| \quad (7)$$

$$\vec{X}(t+1) = \overrightarrow{X} - \vec{A} \cdot \overrightarrow{D} \quad (8)$$

In which  $\overrightarrow{X_{rand}}$  is a vector of position arbitrarily drawn from the existing population (a random whale).

Figure 11 illustrates a few of the different places that might exist in the vicinity of a specific solution that has an  $\bar{A}$  value greater than 1.

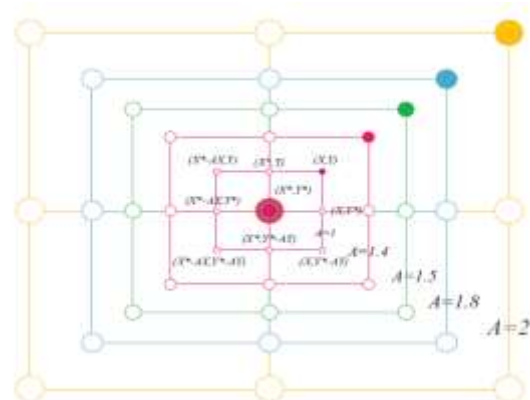


**Figure 11: WOA algorithm's Exploration mechanism.**

The algorithm of WOA begins with a collection of feasible solutions. Each time a new iteration is run, the search agents compare their results to a previously picked search agent or the best solution found up until now. The variable's value is brought down from 2 to 0 to accomplish exploitation and exploration. To adjust the location of the search agents, a stochastic search agent will be picked if  $|A|$  is more than 1, and the optimal solution will be chosen whenever  $|A|$  is less than 1. WOA can switch between circular and spiral movement-based p-values. In conclusion, the WOA algorithm is stopped when a termination requirement is successfully met.

Figure 12 shows the WOA algorithm's pseudo code. According to WOA's conceptual framework, it is possible to contemplate it as a planetary optimizer. In addition to this, the hyper-cube technique that has been described creates a search space close to the optimal solution, which then makes it possible for other search agents to make utilization of the most remarkable record that is now held within that region. It is possible to seamlessly transition between exploitation and exploration by varying the search vector  $A$ . By reducing  $A$ ; some iterations are allocated to exploration ( $|A| \geq 1$ ), while the remainder is committed to exploitation ( $|A| < 1$ ). It is remarkable because WOA only has two key internal settings that may be manipulated ( $A$  and  $C$ ).

```

Initialize the whales population  $X_i$  ( $i = 1, 2, \dots, n$ )
Calculate the fitness of each search agent
 $X^*$  = the best search agent
while ( $i < \text{maximum number of iterations}$ )
  for each search agent
    Update  $a, A, C, L$  and  $p$ 
    if  $i \geq 0.5$ 
      if  $f_2(A) < f_1$ 
        Select a random search agent ( $X_{rand}$ )
        Update the position of the current search agent by the Eq. (2.8)
      end if
    else if  $i \geq 0.5$ 
      Update the position of the current search by the Eq. (2.5)
    end if
  end for
  Check if any search agent goes beyond the search space and amend it
  Calculate the fitness of each search agent
  Update  $X^*$  if there is a better solution
   $i = i + 1$ 
end while
return  $X^*$ 

```

**Figure 12: WOA algorithm's pseudo-code.**

We built an elementary form of the WOA algorithm to limit the number of heuristics and input variables. While mutation and other evolutionary processes could have been contained within the WOA framework to imitate the behavior of humpback whales, ultimately, we chose not to provide them because we intended to replicate the humpback whales' behavior completely. It is possible, nevertheless, that continued studies may examine hybridization using evolutionary search algorithms.

#### 4. Results and Discussion

To replicate the CL of a housing complex, two metaheuristic algorithms, notably WOA, are used to improve the MLP neural network. The MLP and WOA-MLP techniques are conceived and written using MATLAB software. To train the suggested networks, 768 samples were employed, each with one of the eight previously specified individual variables affecting CL in the buildings. This data is split 80/20 between training the networks and evaluating the generalizability of the WOA-MLP and MLP approaches using the other 154 records.

The Weka instrument, a piece of open-source software with constellations of several different machine-learning methods, was used to conduct the comparison simulations. Standard deviation criteria, namely,  $R^2$  and RMSE, were utilized to evaluate the created model performance. Tables 1 to 3 and Figs. 13 to 18 provide the results of the suggested algorithm's performance regarding the cooling load.

**Table 1. Network result variations on the basis of the neurons' number in each hidden layer**

neurons number in each hidden layer	Network results				Scoring		Total score	RANK
	RMSE <sub>total</sub>	RMSE <sub>train</sub>	RMSE <sub>test</sub>	MSE <sub>total</sub>	RMSE <sub>train</sub>	RMSE <sub>test</sub>		
1	0.455	0.445	0.452	6	5	5	16	6
2	0.364	0.355	0.361	9	9	9	27	2
3	0.246	0.231	0.242	10	10	10	30	1
4	1.073	1.058	1.069	1	1	1	3	10
5	0.458	0.427	0.449	5	7	6	18	5
6	0.476	0.498	0.483	4	4	4	12	7
7	0.402	0.403	0.402	8	8	8	24	3
8	1.000	0.971	0.991	2	2	2	6	9
9	0.430	0.430	0.430	7	6	7	20	4
10	0.797	0.811	0.801	3	3	3	9	8

#### 4.1. Accuracy Indicators

Specifically, as shown in Eqs. (9) and (10), two RMSE and  $R^2$  precision criteria are developed to

compare these two methods. Interestingly, several researchers have employed these indexes in their investigations [105, 106]. Following this, a lengthy experimentation process is implemented

to arrive at the most effective configuration for the models. The application of every single model follows this to provide accurate predictions of HL and CL.

$$RMSE = \sqrt{\frac{1}{U} \sum_{i=1}^U [(S_{i_{observed}} - S_{i_{predicted}})^2]} \quad (9)$$

$$R^2 = 1 - \frac{\sum_{i=1}^U (S_{i_{predicted}} - S_{i_{observed}})^2}{\sum_{i=1}^U (S_{i_{observed}} - \bar{S}_{observed})^2} \quad (10)$$

$S_i$  observed and anticipated designating the well-organized building's genuine and expected CL values in that order. The occurrences' number is denoted by the letter U, while the mean of the authentic values of CL is denoted by the letter  $\bar{S}_{observed}$ .

## 4.2. Network Optimization

Soft computing approaches have various variables that might affect their performance. The number of processing units is the one that has the most impact among these many factors. With the help of an experimentation approach, the most suitable MLP and WOA-MLP network structures are found hereunder. As a result, several structures were created and put through rigorous RMSE testing. To construct the MLP, a backpropagation-based network with ten distinct neuron densities and one hidden layer was created. Surprisingly, the Levenberg-Marquardt (LM) training method maps the connection between the freestanding and responsible variables. This strategy was chosen because it performs better than traditional gradient descent methods. According to the findings of the sensitivity study, the MLP network with four hidden layer nodes provides the most precise estimation of the CL output. As a result, the computed RMSE for CL forecasting is 3.85. In the end, the structure of the top-tier MLP may be described using the notation  $8 \times 4 \times 2$ , which signifies that there are correspondingly 2, 4, and 8 computational neurons in the output, hidden, and input layers. These ensembles are created by using a WOA-MLP algorithm on this network.

In terms of the WOA-MLP model, an iterative experimentation procedure is utilized to calculate the optimal values for the WOA algorithm's variables. Optimization methods have several factors that need to be tinkered with to maximize

their effectiveness. When using a population-based method like WOA, the population size is the foremost aspect to consider. In addition to this, the learning process is significantly influenced by the epochs' total number, also known as repetition. Put another way, the model's population size has been optimized in the first place. To accomplish this goal, ten distinct swarm sizes and within one thousand repetitions are put to the test. According to the findings in Fig. 13, the WOAMLP algorithm achieves its maximum accuracy when applied to networks with a swarm size of 500.

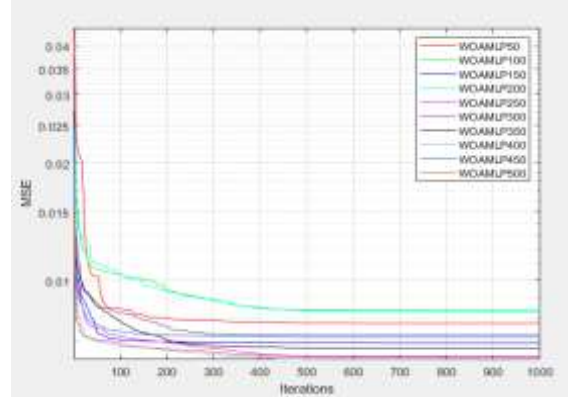


**Figure 13: Best fit proposed structures with various WOA population sizes between 50-500**

According to what can be observed, the WOA-MLP ensemble has the most excellent converging curves (the minimum RMSE by the time the process is complete) when using the population size of 500. Figure 14 displays the MSE calculated with the p-value appropriate for a population size of 500 (0.5, 0.6, 0.7, 0.8, 0.9, 0.1, 1.1, 1.2, 1.3, and 1.4). The minimum MSE indicates the precise outcome and provides the most outstanding value. This graphic shows that the MSE is at its lowest for the value of p equal to 1.3, indicating that this particular value yields the best precise outcomes when forecasting CL. Figure 14 shows that the greatest MSE, p=1.3, caused the most inaccurate results.

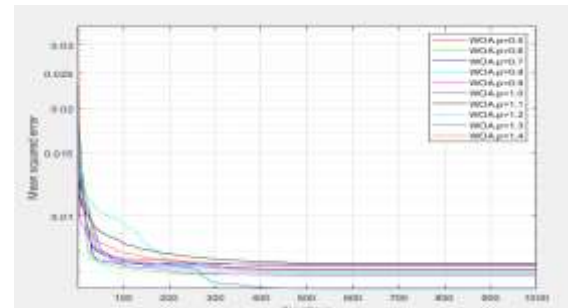
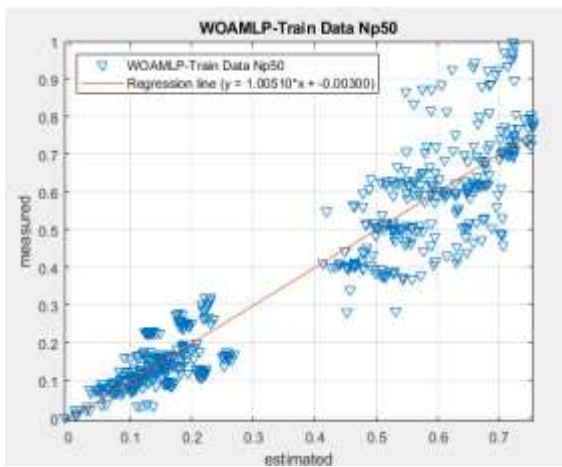
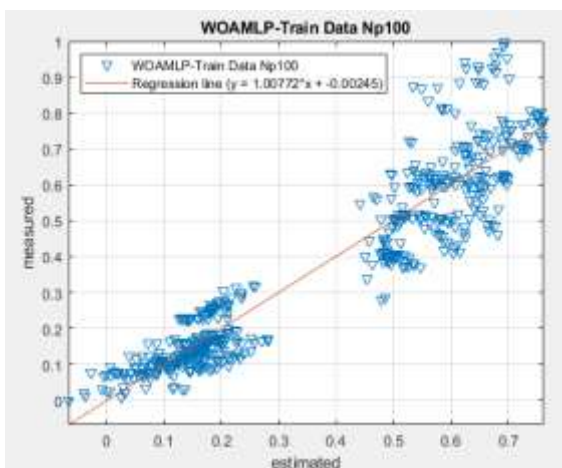


**Figure 14: Best fit suggested 500 architectures with different WOA p-values between 0.5 to 1.4**

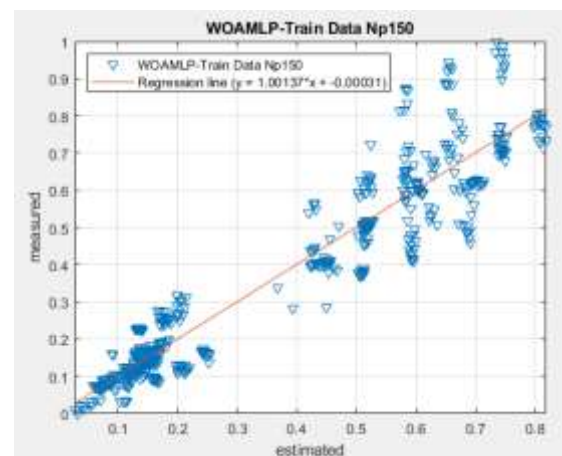
This section assesses the validity of the built methods by comparing the anticipated and observed values of cooling load (CL). RMSE and  $R^2$  were determined as the error criterion to quantify the efficiency error level for each of the testing and training samples. Other WOA values ( $p=0.5, 0.6, 0.7, 0.8, 0.9, 0.1, 1.1, 1.2, 1.3$ , and  $1.4$ ) were deliberately tweaked consistent with earlier findings or by trial-and-error. After that, estimates of the CL are derived using these models. Figures 15 and 16 show a graphic representation of the errors for the testing and training stages and the relationship between the existing CLs and the ones anticipated in every model. The extraction of  $R^2$  and RMSSE values from Figs. 15 and 16 yield Table 2, the sum of all regressions, and the optimum population size is displayed on the word of its ordering. Table 2 also presents that a swarm size of 500 had the most incredible precision, with  $R^2$  amount of 0.95021 and 0.95155 for the testing and training phases.



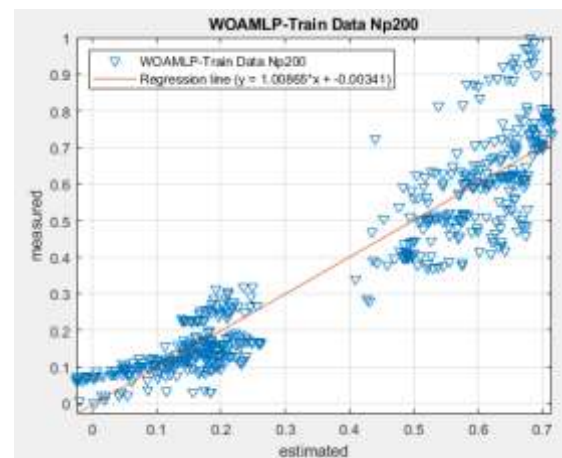
(a) WOAMLP train Np=50



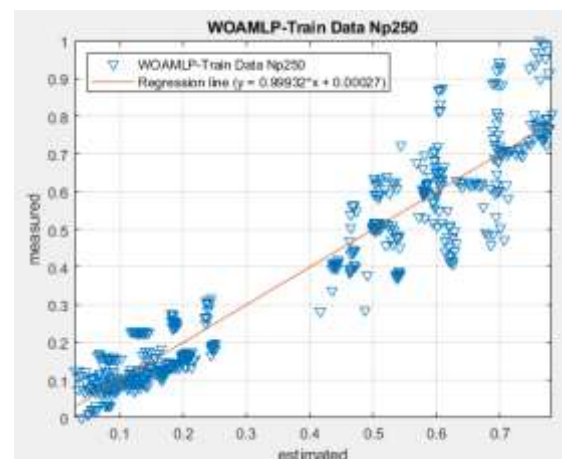
(b) WOAMLP train Np=100



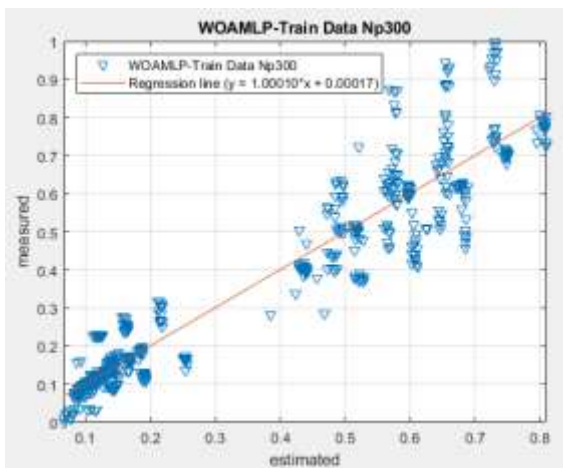
(c) WOAMLP train Np=150



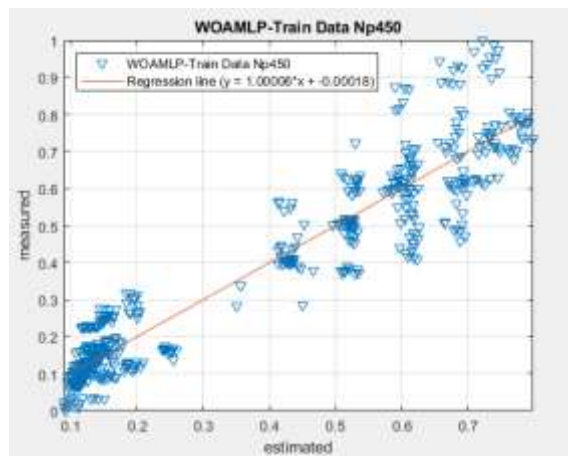
(d) WOAMLP train Np=200



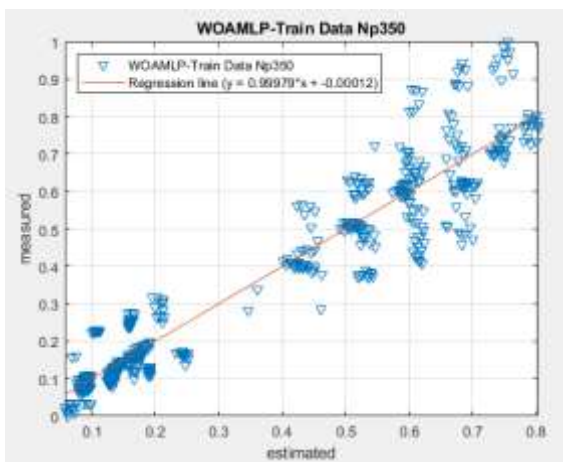
(e) WOAMLP train Np=250



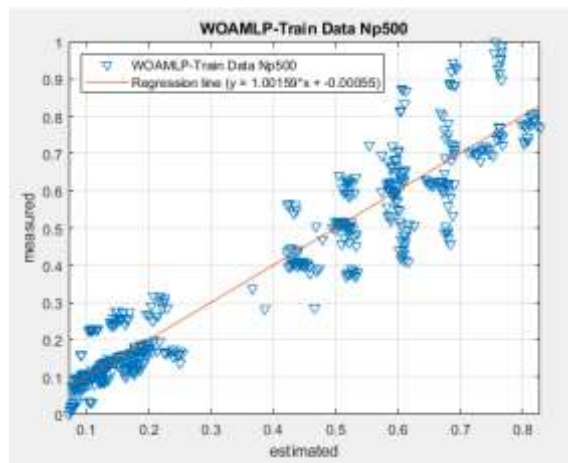
(f) WOAMLP train Np=300



(i) WOAMLP train Np=450

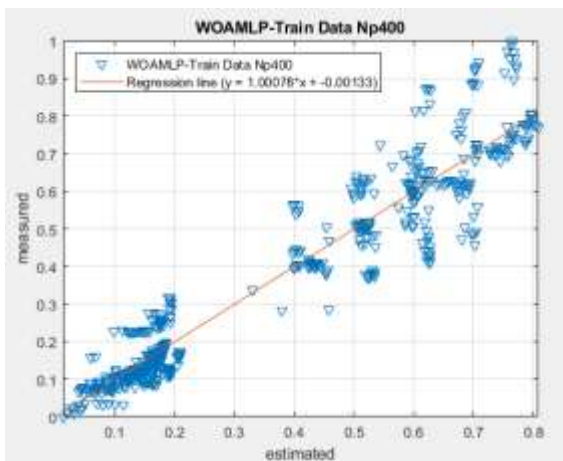


(g) WOAMLP train Np=350

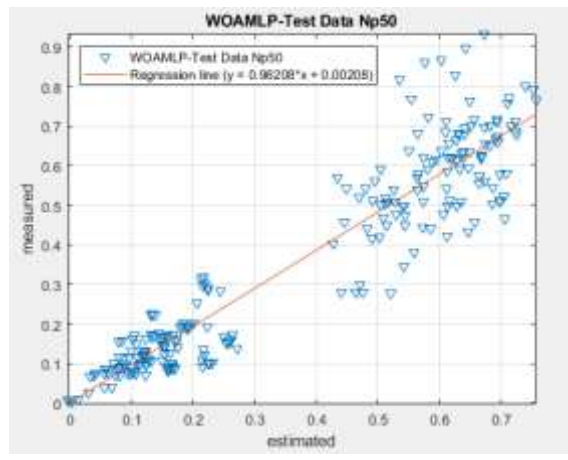


(j) WOAMLP train Np=500

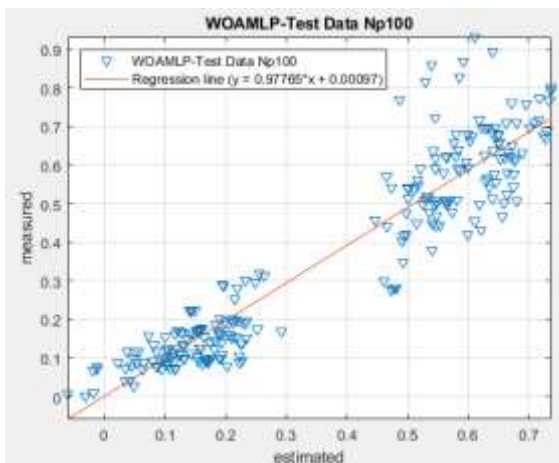
**Figure 15:** The precise of the WOAMLP training dataset in the first optimization phase, after changing the population size between 50 and 500



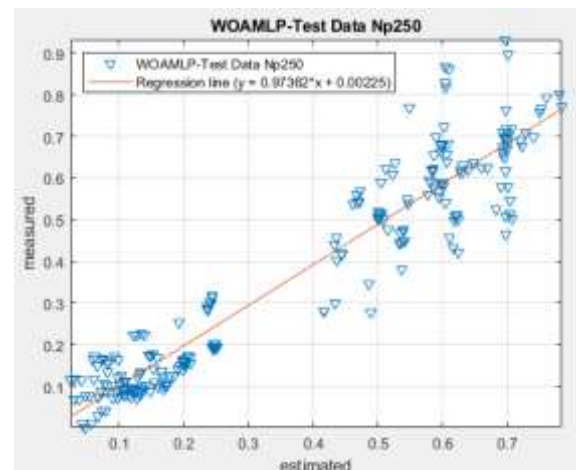
(h) WOAMLP train Np=400



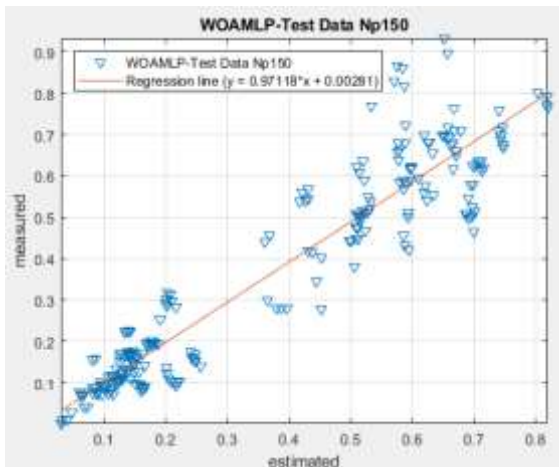
(a) WOAMLP train Np=50



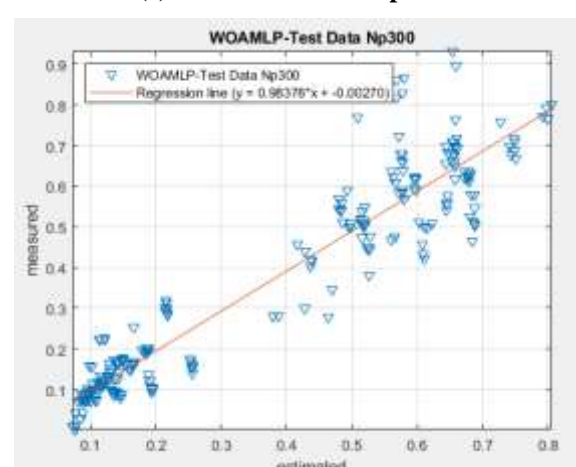
(b) WOAMLP train Np=100



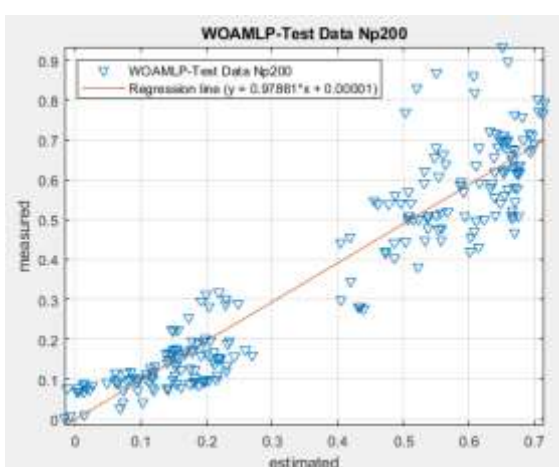
(e) WOAMLP train Np=250



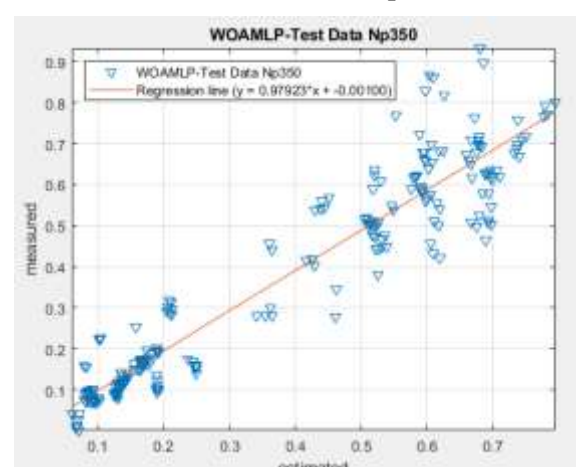
(c) WOAMLP train Np=150



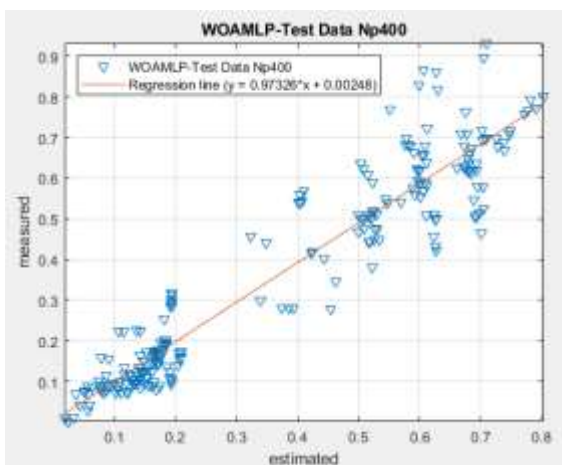
(f) WOAMLP train Np=300



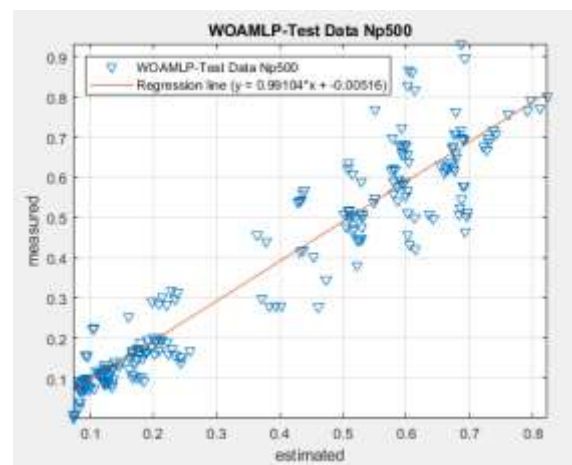
(d) WOAMLP train Np=200



(g) WOAMLP train Np=350

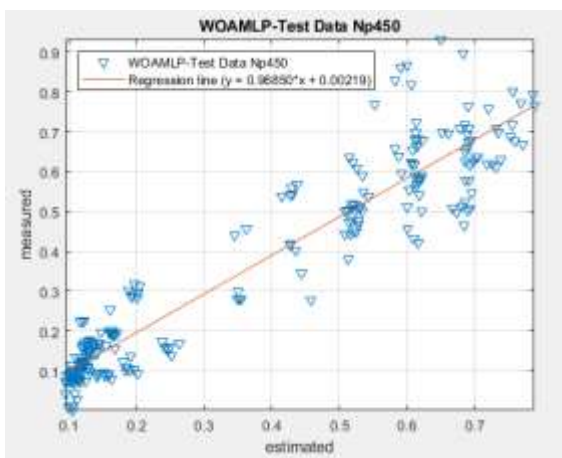


(h) WOAMLP train Np=400



(j) WOAMLP train Np=500

**Figure 16: The precise of the WOAMLP testing dataset in the first optimization phase, after changing the population size between 50 and 500**

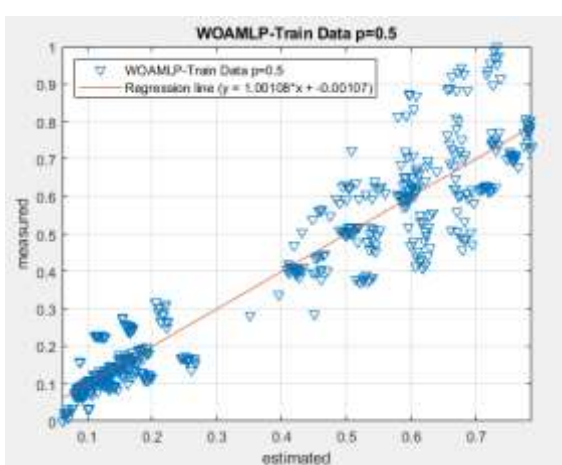
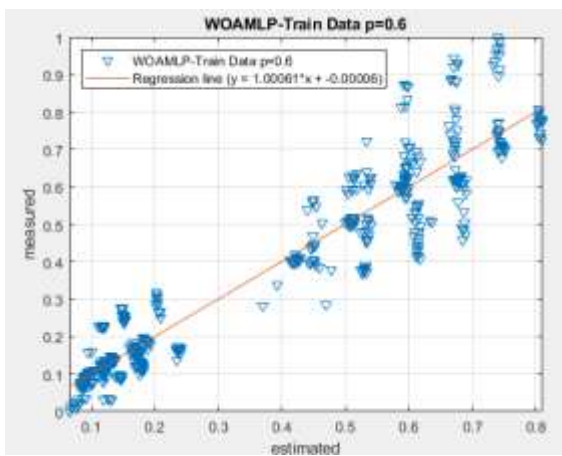
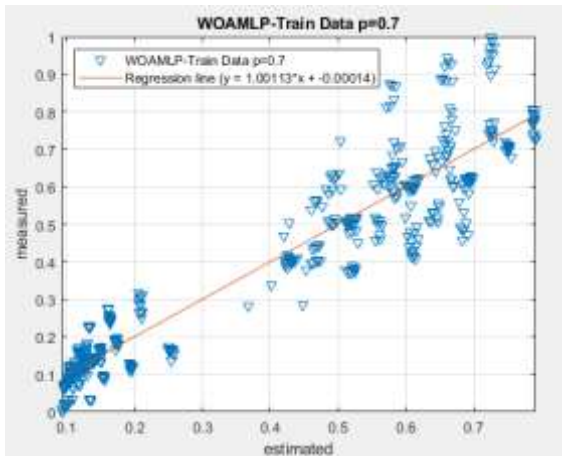
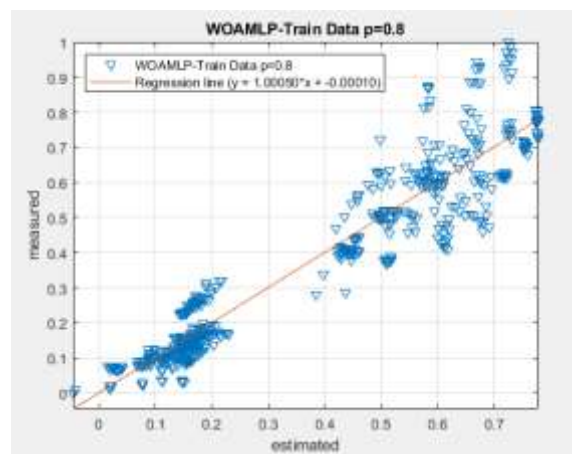
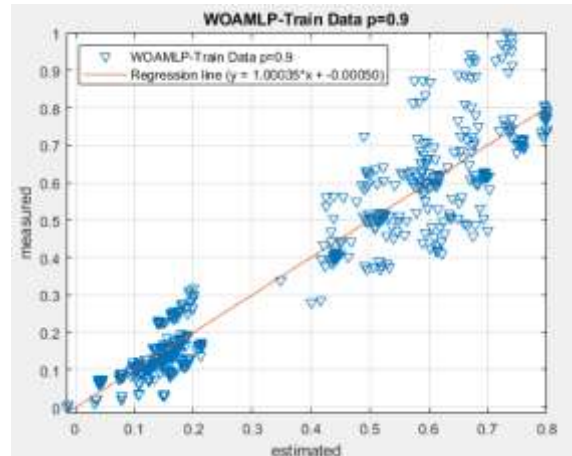
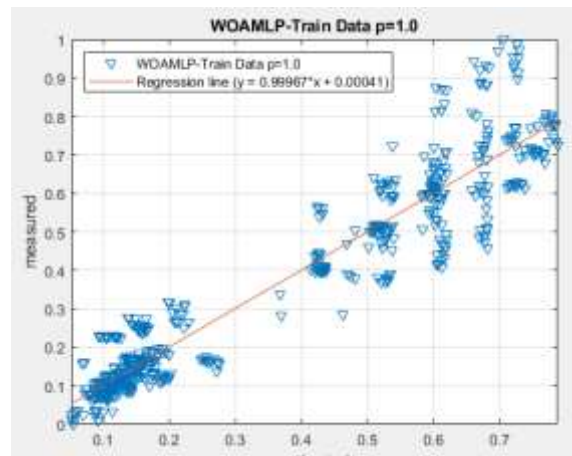


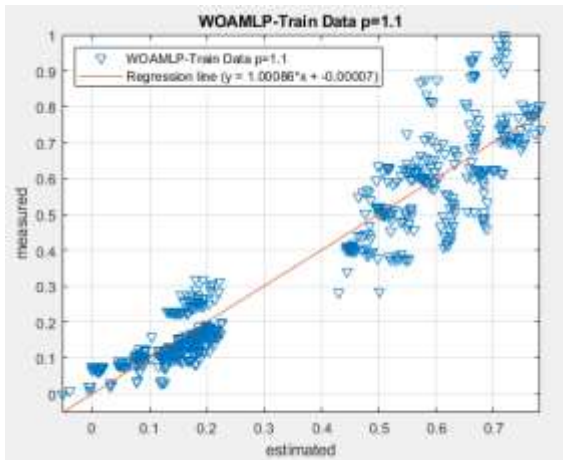
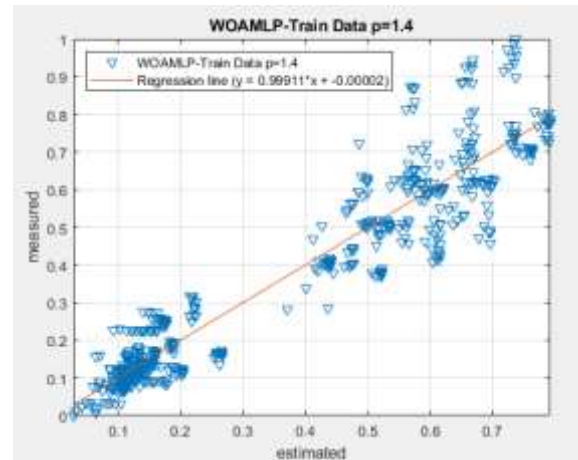
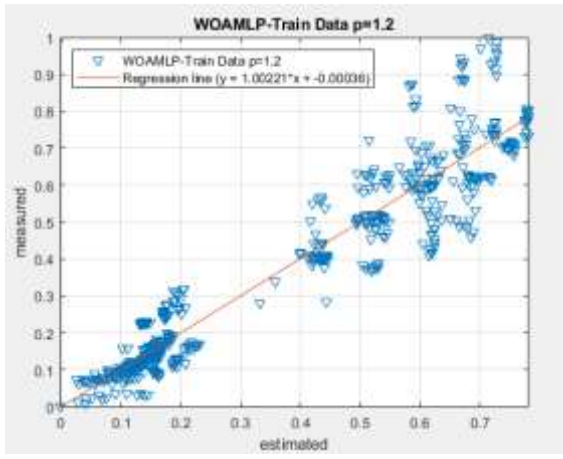
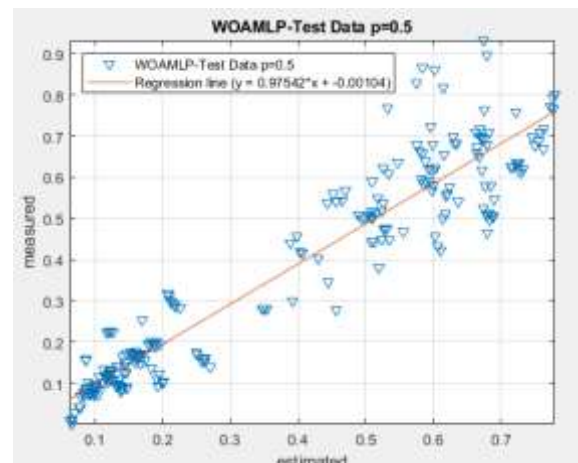
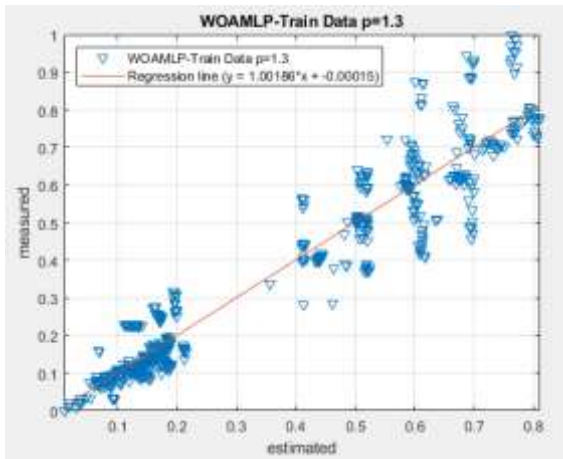
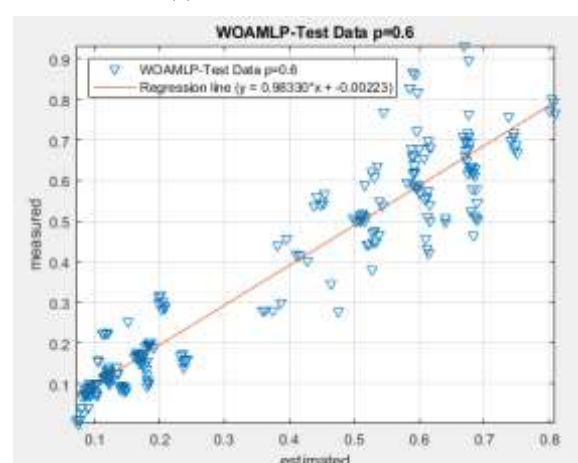
(i) WOAMLP train Np=450

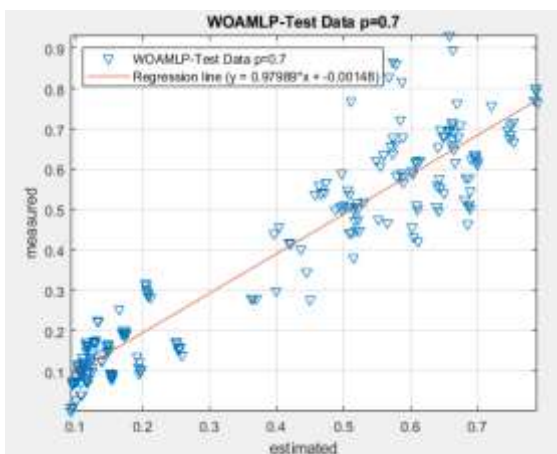
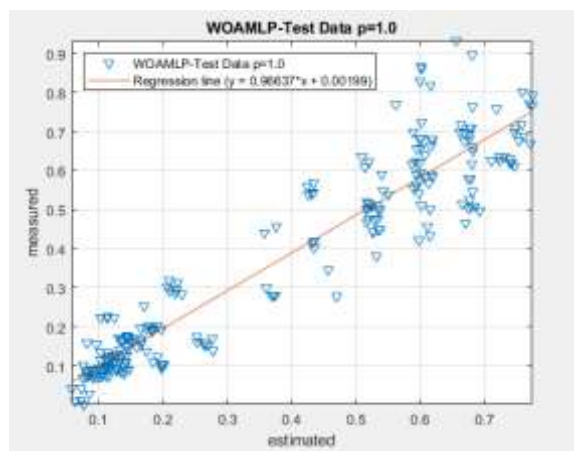
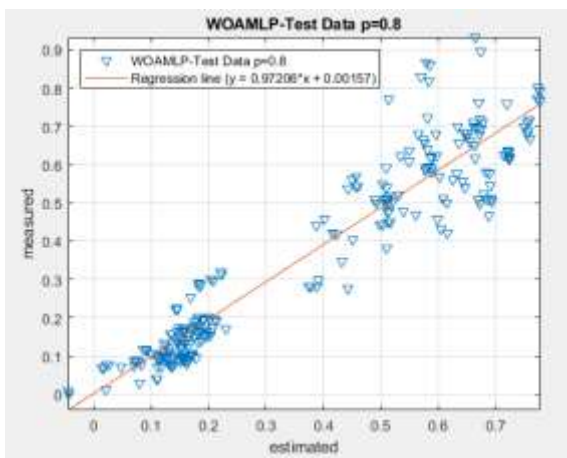
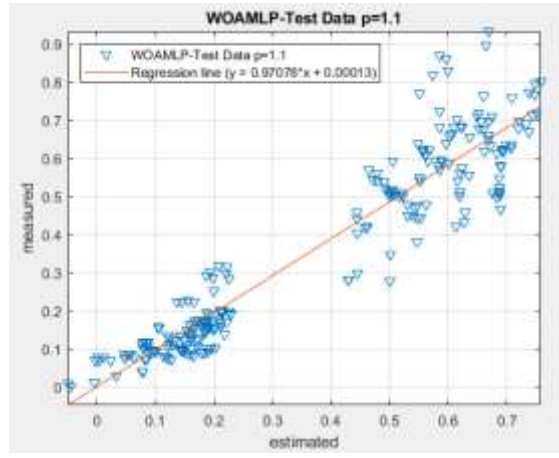
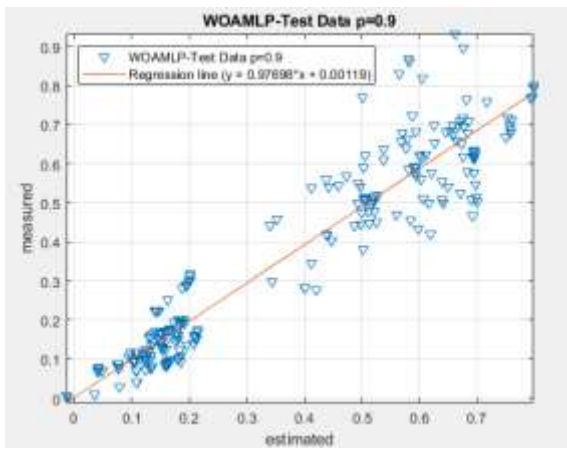
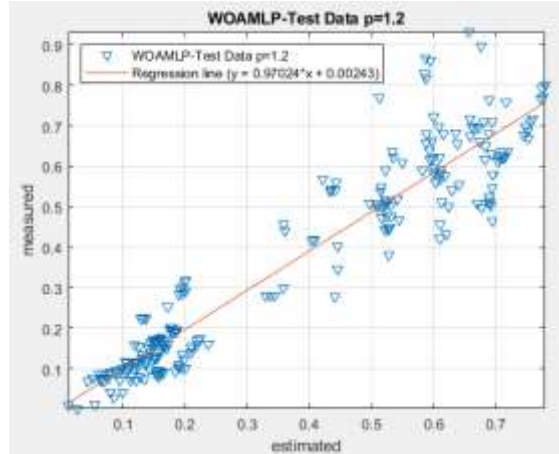
The most excellent precision is found for a population size of 500 when  $R^2$  values (namely, the least RMSE after the procedure) are considered.  $R^2$  is shown graphically in Figures 15 and 16 for a population of 500 throughout the testing and training phases, with p values equal to 0.5, 0.6, 0.7, 0.8, 0.9, 0.1, 1.1, 1.2, 1.3, and 1.3. It was previously indicated that Table 3 can be derived from the  $R^2$  and RMSE values related to Figs. 17 and 18; this is a compilation of all regressions, and the most outstanding possible result is displayed based on its ordering. The p-value equal to 1.3 produces the most excellent  $R^2$  value, as seen in Figs. 17 and 18, as well as Table 3 (0.95212 and 0.94792 for training and testing, respectively).

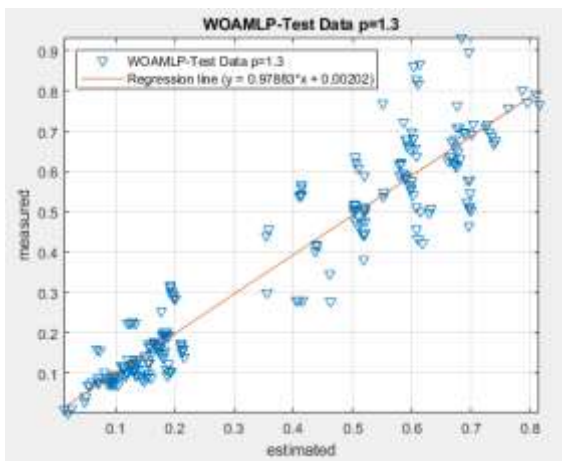
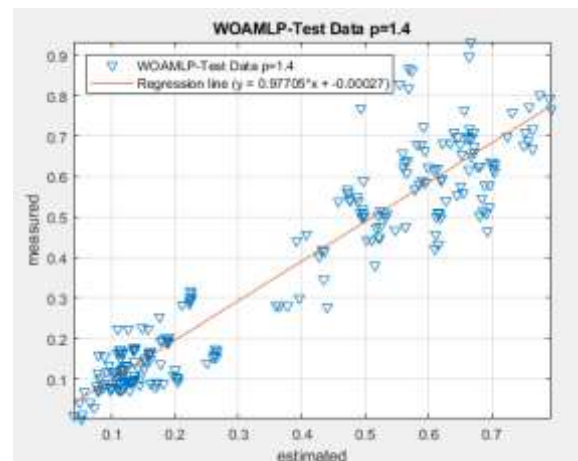
**Table 2. The results of the network for the WOAMLP with different population sizes**

Swarm size	Training dataset		Testing dataset		Scoring		Total Score	Rank		
	RMSE	$R^2$	RMSE	$R^2$	Training	Testing				
50	0.08815	0.94043	0.08678	0.93693	3	3	2	2	10	8
100	0.0913	0.93595	0.08699	0.93661	2	2	1	1	6	10
150	0.08311	0.94723	0.0835	0.94176	6	6	4	4	20	5
200	0.0917	0.93537	0.08395	0.94111	1	1	3	3	8	9
250	0.07991	0.95132	0.07903	0.948	8	8	8	8	32	3
300	0.08516	0.94451	0.08076	0.94562	4	4	6	6	20	5
350	0.08194	0.94875	0.07886	0.94823	7	7	9	9	32	3
400	0.07914	0.95228	0.07944	0.94743	10	10	7	7	34	2
450	0.08459	0.94528	0.08232	0.94343	5	5	5	5	20	5
500	0.07973	0.95155	0.07737	0.95021	9	9	10	10	38	1

(a) WOAMLP train  $\alpha=0.5$ (b) WOAMLP train  $\alpha=0.6$ (c) WOAMLP train  $\alpha=0.7$ (d) WOAMLP train  $\alpha=0.8$ (e) WOAMLP train  $\alpha=0.9$ (f) WOAMLP train  $\alpha=1.0$

(g) WOAMLP train  $\alpha=1.1$ (j) WOAMLP train  $\alpha=1.4$ (h) WOAMLP train  $\alpha=1.2$ (a) WOAMLP test  $\alpha=0.5$ (i) WOAMLP train  $\alpha=1.3$ (b) WOAMLP test  $\alpha=0.6$

(c) WOAMLP test  $\alpha=0.7$ (f) WOAMLP test  $\alpha=1.0$ (d) WOAMLP test  $\alpha=0.8$ (g) WOAMLP test  $\alpha=1.1$ (e) WOAMLP test  $\alpha=0.9$ (h) WOAMLP test  $\alpha=1.2$

(i) WOAMLP test  $\alpha=1.3$ (j) WOAMLP test  $\alpha=1.4$ 

**Figure 18: Testing accuracy for the proposed structure having different WOA p parameters varied from 0.5 to 1.4**

**Table 3. The network results for the WOAMLP have different p-values**

Swam size	Training dataset		Testing dataset		Scoring		Total Score	Rank
	RMSE	R <sup>2</sup>	RMSE	R <sup>2</sup>	Training	Testing		
0.5	0.08403	0.94602	0.07993	0.94676	5	5	8	26
0.6	0.08287	0.94754	0.07859	0.94858	8	8	10	36
0.7	0.08558	0.94395	0.08184	0.94412	2	2	3	10
0.8	0.0838	0.94633	0.08073	0.94567	6	6	6	24
0.9	0.08275	0.9477	0.08046	0.94604	9	9	7	32
1	0.08443	0.94549	0.08131	0.94486	4	4	4	16
1.1	0.08601	0.94338	0.08214	0.9437	1	1	2	6
1.2	0.08325	0.94705	0.08077	0.9456	7	7	5	24
1.3	0.07926	0.95212	0.07909	0.94792	10	10	9	38
1.4	0.08529	0.94435	0.08221	0.94359	3	3	1	9

## 5. Discussion

The versatility of the hybrid load forecasting approach is shown in this research. For the most part, the building model is utilized to gather data on cooling loads. It is essential to rebuild the building method and update the building database whenever it is altered. Since this article concentrates on the influence of external disturbances on the load predicting method, the proposed hybrid method has postulated that the structures' internal disturbances are stationary.

When the building method is being created, one may thus circumvent the problem of the constantly shifting internal disturbances and save themselves from potential harm. In residential structures, the cooling load might be affected by internal disturbances; hence, the suggested hybrid load forecasting approach is appropriate. It is possible to do dynamic load forecasting for HVAC systems by leveraging an available database to construct an extrapolation model for

residential buildings. You must include the input of internal disturbance variables into the suggested hybrid load forecasting approach, as well as create two models of the working day load predicting and the holiday load predicting if you would like to utilize it for public structures like marketable buildings whose loads are heavily impacted by internal disturbances. Therefore, it applies to most types of municipal buildings.

In several engineering measures, intelligent models are primarily recognized to be superior to conventional and experimental procedures. In addition to their high degree of certainty, these models' simplicity of execution is a crucial factor in their widespread adoption. Concerning energy efficiency studies, there may be specific difficulties connected with employing methodologies of forward modeling and widely used software for simulation (various precision of simulation). Indirect evaluation models like those presented in this study are desirable to avoid expensive and damaging methods. Metaheuristic tools emphasize this even more when used to construct an ideal methodology. In other words, optimizing algorithms results in competent ensembles that function in perfect circumstances.

- a) If you plan to build a new building, the proposed model may help you determine how much thermal load you will need based on the size and other aspects of the structure. When designing and installing HVAC systems, this approach will be helpful for engineers and building owners.
- b) One option for initial support in rebuilding projects would be to help with optimal architectural design and tune the layout via input parameters. When analyzing the thermal load behavior, looking at each input parameter individually is also feasible. The WOA-MLP, on the other hand, accurately predicts it. It is also possible to use this technique for real-world buildings.
- c) This approach, known as the two-phase method, does the analysis in the first phase, just as the prior study did, and then chooses the population size that would provide the best results. The RMSE and  $R^2$  values for this population size are the lowest and highest, respectively, and their forecasting seems to be the most precise. As a result of that particular section's inclusion, this piece stands apart from the others. Examining the optimal swarm size from the previous step is the focus of the

second phase. In this manner, multiple distinct values have been explored for the  $p$  parameter (which was covered in part before this one), and the one that has been retrieved has the lowest RMS and the highest  $R^2$  value. It is also important to note that the recommended method was provided as an explicit mathematical formula, which, compared to the GUI form in MATLAB, is more straightforward to utilize and more user-friendly.

Nevertheless, many investigations have successfully used machine learning technologies to correctly forecast the thermal loads of buildings utilized for aims other than residential, including commercial and industrial [107]. There is a connection between the majority of these concepts and the information. There are a few things to remember when comparing these findings to those obtained with normalized data. These simulations must be analyzed to determine which data sets are most suited. Another advantage of optimizing the number of inputs is that it reduces the complexity of the procedure, reducing the number of variables that must be optimized. When the HL and CL are combined, the issue becomes a two-target simulation, and the advantage should be weighed against the greater sophistication. Another possible topic is using many architectural styles within the same research project. Using this method, the model may be utilized for a wide range of different architectural applications. In conclusion, it is strongly suggested that future research compare efforts to identify the most effective algorithm when coupled with ANN or other intelligent tools.

## 6. Conclusions

Over the last several years, novel approaches for determining buildings' energy usage have been developed. Metaheuristic algorithms were used in this article to solve the imperfections of the backpropagation techniques. The green building's CL was estimated by synthesizing a standard MLP utilizing a WOA-MLP. To do this, eight key energy factors, such as roof area, relative compactness, surface area, orientation, glazing area, overall height, wall area, and glazing area distribution, were addressed as the networks' inputs. Different building environment was used to model and assess 768 structures, considering twelve four-glazing regions, distinct buildings, four orientations, and five distribution scenarios.

Eighty percent (614 records) were used to train the MLP and WOA-MLP models, while the residual twenty percent (154 records) were used to assess their effectiveness. The suggested models were implemented under their ideal circumstances, and two well-known statistical criteria, RMSE and  $R^2$ , were utilized to evaluate the correctness of every single technique. We found that methods based on artificial intelligence have the potential to be an effective solution to the problem of assessing the cooling loads of buildings. Both pattern learning and prediction are improved significantly when the WOA calibrates the ANN's computational parameters (that is, its biases and weights). According to the estimated RMSE and  $R^2$  (0.07973 and 0.07737) and (0.95155 and 0.95021) during training and testing, a sample size of 500 people yielded the most precise findings. The p value was changed from 0.5 to 1.3 for a population size of 500, and the most remarkable conclusion was drawn when p was set to 1.3. This value produced an  $R^2$  value of 0.95212 and 0.94792 and an RMSE value of 0.07926 and 0.07909 for the training and testing stages, respectively.

## 7. References

[1] Al-Homoud, Mohammad Saad, Computer-aided building energy analysis techniques, *Building and Environment*, 36 (2001) 421-433,

[2] Yang, Wenjie, Yue Zhao, Dong Wang, Huihui Wu, Aijun Lin, Li He, Using principal components analysis and IDW interpolation to determine spatial and temporal changes of surface water quality of Xin'anjiang river in Huangshan, China, *International journal of environmental research and public health*, 17 (2020) 2942,

[3] Zuo, Xue, Mingyu Dong, Fengkai Gao, Shiming Tian, The modeling of the electric heating and cooling system of the integrated energy system in the coastal area, *Journal of Coastal Research*, 103 (2020) 1022-1029,

[4] Moayedi, Hossein, Mesut Gör, Zongjie Lyu, Dieu Tien Bui, Herding Behaviors of grasshopper and Harris hawk for hybridizing the neural network in predicting the soil compression coefficient, *Measurement*, 152 (2020) 107389,

[5] Ahmadi-Karvigh, Simin, Ali Ghahramani, Burcin Becerik-Gerber, Lucio Soibelman, Real-time activity recognition for energy efficiency in buildings, *Applied energy*, 211 (2018) 146-160,

[6] Bibri, Simon Elias, John Krogstie, Smart sustainable cities of the future: An extensive interdisciplinary literature review, *Sustainable cities and society*, 31 (2017) 183-212,

[7] McQuiston, Faye C, Jerald D Parker, Jeffrey D Spitler, *Heating, ventilating, and air conditioning: analysis and design*, John Wiley & Sons, 2004.

[8] Chen, Yizhong, Li He, Yanlong Guan, Hongwei Lu, Jing Li, Life cycle assessment of greenhouse gas emissions and water-energy optimization for shale gas supply chain planning based on multi-level approach: Case study in Barnett, Marcellus, Fayetteville, and Haynesville shales, *Energy conversion and management*, 134 (2017) 382-398,

[9] Chen, Yizhong, Li He, Jing Li, Shiyue Zhang, Multi-criteria design of shale-gas-water supply chains and production systems towards optimal life cycle economics and greenhouse gas emissions under uncertainty, *Computers & chemical engineering*, 109 (2018) 216-235,

[10] Chen, Yizhong, Jing Li, Hongwei Lu, Pengdong Yan, Coupling system dynamics analysis and risk aversion programming for optimizing the mixed noise-driven shale gas-water supply chains, *Journal of Cleaner Production*, 278 (2021) 123209,

[11] Cheng, Xi, Li He, Hongwei Lu, Yizhong Chen, Lixia Ren, Optimal water resources management and system benefit for the Marcellus shale-gas reservoir in Pennsylvania and West Virginia, *Journal of Hydrology*, 540 (2016) 412-422,

[12] Han, Xiaoqu, Dan Zhang, Junjie Yan, Shuran Zhao, Jiping Liu, Process development of flue gas desulphurization wastewater treatment in coal-fired power plants towards zero liquid discharge: Energetic, economic and environmental analyses, *Journal of Cleaner Production*, 261 (2020) 121144,

[13] He, Li, Yizhong Chen, Honghai Zhao, Peipei Tian, Yuxuan Xue, Liang Chen, Game-based analysis of energy-water nexus for identifying environmental impacts during Shale gas operations under stochastic input, *Science of The Total Environment*, 627 (2018) 1585-1601,

[14] Li, Zhi-Guo, Han Cheng, Tian-Yao Gu, Research on dynamic relationship between natural gas consumption and economic growth in China, *Structural Change and Economic Dynamics*, 49 (2019) 334-339,

[15] Liu, Enbin, Liuxin Lv, Yang Yi, Ping Xie, Research on the steady operation optimization model of natural gas pipeline considering the combined operation of air coolers and compressors, *IEEE access*, 7 (2019) 83251-83265,

[16] Su, Zhongya, Enbin Liu, Yawen Xu, Ping Xie, Chen Shang, Qiyong Zhu, Flow field and noise characteristics of manifold in natural gas transportation station, *Oil & Gas Science and Technology–Revue d'IFP Energies nouvelles*, 74 (2019) 70,

[17] He, Li, Jing Shen, Yang Zhang, Ecological vulnerability assessment for ecological conservation

and environmental management, *Journal of environmental management*, 206 (2018) 1115-1125,

[18] Lu, Hongwei, Peipei Tian, Li He, Evaluating the global potential of aquifer thermal energy storage and determining the potential worldwide hotspots driven by socio-economic, geo-hydrologic and climatic conditions, *Renewable and Sustainable Energy Reviews*, 112 (2019) 788-796,

[19] Tian, Peipei, Hongwei Lu, Wei Feng, Yanlong Guan, Yuxuan Xue, Large decrease in streamflow and sediment load of Qinghai-Tibetan Plateau driven by future climate change: A case study in Lhasa River Basin, *Catena*, 187 (2020) 104340,

[20] Zhang, Ke, Gebdang B Ruben, Xin Li, Zhijia Li, Zhongbo Yu, Jun Xia, Zengchuan Dong, A comprehensive assessment framework for quantifying climatic and anthropogenic contributions to streamflow changes: A case study in a typical semi-arid North China basin, *Environmental Modelling & Software*, 128 (2020) 104704,

[21] Chen, Huazhou, An Chen, Lili Xu, Hai Xie, Hanli Qiao, Qinyong Lin, Ken Cai, A deep learning CNN architecture applied in smart near-infrared analysis of water pollution for agricultural irrigation resources, *Agricultural Water Management*, 240 (2020) 106303,

[22] Zhang, Wei, Parameter adjustment strategy and experimental development of hydraulic system for wave energy power generation, *Symmetry*, 12 (2020) 711,

[23] Bui, Xuan-Nam, Hossein Moayedi, Ahmad Safuan A Rashid, Developing a predictive method based on optimized M5Rules-GA predicting heating load of an energy-efficient building system, *Engineering with Computers*, 36 (2020) 931-940,

[24] Gao, Wei, Jalal Alsarraf, Hossein Moayedi, Amin Shahsavari, Hoang Nguyen, Comprehensive preference learning and feature validity for designing energy-efficient residential buildings using machine learning paradigms, *Applied Soft Computing*, 84 (2019) 105748,

[25] Guo, Zhanjun, Hossein Moayedi, Loke Kok Foong, Mehdi Bahiraei, Optimal modification of heating, ventilation, and air conditioning system performances in residential buildings using the integration of metaheuristic optimization and neural computing, *Energy and Buildings*, 214 (2020) 109866,

[26] Jun, Zhang, Zhang Kanyu, A particle swarm optimization approach for optimal design of PID controller for temperature control in HVAC, 2011 Third International Conference on Measuring Technology and Mechatronics Automation, IEEE, 2011, pp. 230-233.

[27] Moayedi, Hossein, Dieu Tien Bui, Anastasios Dounis, Zongjie Lyu, Loke Kok Foong, Predicting heating load in energy-efficient buildings through

machine learning techniques, *Applied Sciences*, 9 (2019) 4338,

[28] Moayedi, Hossein, Mohammed Abdullahi Mu'azu, Loke Kok Foong, Novel swarm-based approach for predicting the cooling load of residential buildings based on social behavior of elephant herds, *Energy and Buildings*, 206 (2020) 109579,

[29] Ghahramani, Ali, Simin Ahmadi Karvigh, Burcin Becerik-Gerber, HVAC system energy optimization using an adaptive hybrid metaheuristic, *Energy and Buildings*, 152 (2017) 149-161,

[30] Tien Bui, Dieu, Hossein Moayedi, Dounis Anastasios, Loke Kok Foong, Predicting heating and cooling loads in energy-efficient buildings using two hybrid intelligent models, *Applied Sciences*, 9 (2019) 3543,

[31] Zhou, Guofeng, Hossein Moayedi, Mehdi Bahiraei, Zongjie Lyu, Employing artificial bee colony and particle swarm techniques for optimizing a neural network in prediction of heating and cooling loads of residential buildings, *Journal of Cleaner Production*, 254 (2020) 120082,

[32] Ghahramani, Ali, Kenan Zhang, Kanu Dutta, Zheng Yang, Burcin Becerik-Gerber, Energy savings from temperature setpoints and deadband: Quantifying the influence of building and system properties on savings, *Applied Energy*, 165 (2016) 930-942,

[33] Ferreira, PM, AE Ruano, S Silva, EZE Conceicao, Neural networks based predictive control for thermal comfort and energy savings in public buildings, *Energy and buildings*, 55 (2012) 238-251,

[34] Park, JS, Suk Joo Lee, Kee Han Kim, Kyung Woo Kwon, Jae-Weon Jeong, Estimating thermal performance and energy saving potential of residential buildings using utility bills, *Energy and buildings*, 110 (2016) 23-30,

[35] Wang, Zhe, Tianzhen Hong, Mary Ann Piette, Building thermal load prediction through shallow machine learning and deep learning, *Applied Energy*, 263 (2020) 114683,

[36] Zhao, Xuan, Yiming Ye, Jian Ma, Peilong Shi, Hao Chen, Construction of electric vehicle driving cycle for studying electric vehicle energy consumption and equivalent emissions, *Environmental Science and Pollution Research*, 27 (2020) 37395-37409,

[37] Li, Tianyi, Mai Xu, Ce Zhu, Ren Yang, Zulin Wang, Zhenyu Guan, A Deep Learning Approach for Multi-Frame In-Loop Filter of HEVC, *Trans. Img. Proc.*, 28 (2019) 5663-5678, 10.1109/tip.2019.2921877.

[38] Xu, M., T. Li, Z. Wang, X. Deng, R. Yang, Z. Guan, Reducing Complexity of HEVC: A Deep Learning Approach, *IEEE Trans Image Process*, (2018), 10.1109/tip.2018.2847035.

[39] Fu, Xiuwen, Pasquale Pace, Gianluca Alois, Lin Yang, Giancarlo Fortino, Topology optimization against cascading failures on wireless sensor networks using a memetic algorithm, *Computer Networks*, 177 (2020) 107327, <https://doi.org/10.1016/j.comnet.2020.107327>.

[40] Fu, Xiuwen, Yongsheng Yang, Modeling and analysis of cascading node-link failures in multi-sink wireless sensor networks, *Reliab. Eng. Syst. Saf.*, 197 (2020) 106815,

[41] Li, Chengye, Lingxian Hou, Bishundat Yanesh Sharma, Huaizhong Li, ChengShui Chen, Yuping Li, Xuehua Zhao, Hui Huang, Zhennao Cai, Huiling Chen, Developing a new intelligent system for the diagnosis of tuberculous pleural effusion, *Computer Methods and Programs in Biomedicine*, 153 (2018) 211-225, <https://doi.org/10.1016/j.cmpb.2017.10.022>.

[42] Cao, B., J. Zhao, Z. Lv, Y. Gu, P. Yang, S. K. Halgamuge, Multiobjective Evolution of Fuzzy Rough Neural Network via Distributed Parallelism for Stock Prediction, *IEEE Transactions on Fuzzy Systems*, 28 (2020) 939-952, 10.1109/TFUZZ.2020.2972207.

[43] Shi, Kaibo, Jun Wang, Yuanyan Tang, Shouming Zhong, Reliable asynchronous sampled-data filtering of T-S fuzzy uncertain delayed neural networks with stochastic switched topologies, *Fuzzy Sets Syst.*, 381 (2020) 1-25, 10.1016/j.fss.2018.11.017.

[44] Shi, Kaibo, Jun Wang, Shouming Zhong, Yuanyan Tang, Jun Cheng, Non-fragile memory filtering of T-S fuzzy delayed neural networks based on switched fuzzy sampled-data control, *Fuzzy Sets and Systems*, 394 (2020) 40-64, <https://doi.org/10.1016/j.fss.2019.09.001>.

[45] Zhu, Q., Research on Road Traffic Situation Awareness System Based on Image Big Data, *IEEE Intelligent Systems*, 35 (2020) 18-26, 10.1109/MIS.2019.2942836.

[46] Lv, Zhihan, Liang Qiao, Deep belief network and linear perceptron based cognitive computing for collaborative robots, *Applied Soft Computing*, 92 (2020) 106300, <https://doi.org/10.1016/j.asoc.2020.106300>.

[47] Qian, Jiaming, Shijie Feng, Yixuan Li, Tianyang Tao, Jing Han, Qian Chen, Chao Zuo, Single-shot absolute 3D shape measurement with deep-learning-based color fringe projection profilometry, *Optics Letters*, 45 (2020) 1842-1845, 10.1364/OL.388994.

[48] Qiu, Tianshuo, Xin Shi, Jiafu Wang, Yongfeng Li, Shaobo Qu, Qiang Cheng, Tiejun Cui, Sai Sui, Deep Learning: A Rapid and Efficient Route to Automatic Metasurface Design, *Advanced Science*, 6 (2019), 10.1002/advs.201900128.

[49] Hu, L., G. Hong, J. Ma, X. Wang, H. Chen, An efficient machine learning approach for diagnosis of paraquat-poisoned patients, *Comput Biol Med*, 59 (2015) 116-124, 10.1016/j.combiomed.2015.02.003.

[50] Shen, Liming, Huiling Chen, Zhe Yu, Wenchang Kang, Bingyu Zhang, Huaizhong Li, Bo Yang, Dayou Liu, Evolving support vector machines using fruit fly optimization for medical data classification, *Knowledge-Based Systems*, 96 (2016) 61-75, <https://doi.org/10.1016/j.knosys.2016.01.002>.

[51] Zhang, X., M. Fan, D. Wang, P. Zhou, D. Tao, Top-k Feature Selection Framework Using Robust 0-1 Integer Programming, *IEEE Trans Neural Netw Learn Syst*, 32 (2021) 3005-3019, 10.1109/tnnls.2020.3009209.

[52] Zhao, Xuehua, Daoliang Li, Bo Yang, Huiling Chen, Xinbin Yang, Chenglong Yu, Shuangyin Liu, A two-stage feature selection method with its application, *Computers & Electrical Engineering*, 47 (2015) 114-125, 10.1016/j.compeleceng.2015.08.011.

[53] Wang, Mingjing, Huiling Chen, Bo Yang, Xuehua Zhao, Lufeng Hu, Zhen-Nao Cai, Hui Huang, Changfei Tong, Toward an optimal kernel extreme learning machine using a chaotic moth-flame optimization strategy with applications in medical diagnoses, *Neurocomputing*, 267 (2017), 10.1016/j.neucom.2017.04.060.

[54] Wang, Su-Jing, Hui-Ling Chen, Wen-Jing Yan, Yu-Hsin Chen, Xiaolan Fu, Face Recognition and Micro-expression Recognition Based on Discriminant Tensor Subspace Analysis Plus Extreme Learning Machine, *Neural Process. Lett.*, 39 (2014) 25-43, 10.1007/s11063-013-9288-7.

[55] Xia, J., H. Chen, Q. Li, M. Zhou, L. Chen, Z. Cai, Y. Fang, H. Zhou, Ultrasound-based differentiation of malignant and benign thyroid nodules: An extreme learning machine approach, *Comput Methods Programs Biomed*, 147 (2017) 37-49, 10.1016/j.cmpb.2017.06.005.

[56] Abedini, Masoud, Chunwei Zhang, Performance assessment of concrete and steel material models in ls-dyna for enhanced numerical simulation, a state of the art review, *Archives of Computational Methods in Engineering*, 28 (2021) 2921-2942,

[57] Gholipour, Gholamreza, Chunwei Zhang, Asma Alasadat Mousavi, Numerical analysis of axially loaded RC columns subjected to the combination of impact and blast loads, *Engineering Structures*, 219 (2020) 110924,

[58] Liu, Jianjun, Changzhi Wu, Guoning Wu, Xiangyu Wang, A novel differential search algorithm and applications for structure design, *Applied Mathematics and Computation*, 268 (2015) 246-269,

[59] Mou, Ben, Fei Zhao, Qiyun Qiao, Lingling Wang, Haitao Li, Baojie He, Zhiyu Hao, Flexural behavior of beam to column joints with or without an overlying

concrete slab, *Engineering Structures*, 199 (2019) 109616,

[60] Wang, Jianhui, Yunchang Huang, Tao Wang, Chunliang Zhang, Yan hui Liu, Fuzzy finite-time stable compensation control for a building structural vibration system with actuator failures, *Applied Soft Computing*, 93 (2020) 106372,

[61] Wu, Chengke, Peng Wu, Jun Wang, Rui Jiang, Mengcheng Chen, Xiangyu Wang, Critical review of data-driven decision-making in bridge operation and maintenance, *Structure and Infrastructure Engineering*, 18 (2021) 47-70,

[62] Zhang, Chunwei, M Abedini, J Mehrmashhadi, Development of pressure-impulse models and residual capacity assessment of RC columns using high fidelity Arbitrary Lagrangian-Eulerian simulation, *Engineering Structures*, 224 (2020) 111219,

[63] Zhang, Chunwei, Hao Wang, Swing vibration control of suspended structures using the Active Rotary Inertia Driver system: Theoretical modeling and experimental verification, *Structural Control and Health Monitoring*, 27 (2020) e2543,

[64] Chao, Mi, Chen Kai, Zhang Zhiwei, Research on tobacco foreign body detection device based on machine vision, *Transactions of the Institute of Measurement and Control*, 42 (2020) 2857-2871,

[65] Liu, Dong, Shengsheng Wang, Dezhi Huang, Gang Deng, Fantao Zeng, Huijing Chen, Medical image classification using spatial adjacent histogram based on adaptive local binary patterns, *Computers in biology and medicine*, 72 (2016) 185-200,

[66] Xu, Mai, Chen Li, Shanyi Zhang, Patrick Le Callet, State-of-the-art in 360 video/image processing: Perception, assessment and compression, *IEEE Journal of Selected Topics in Signal Processing*, 14 (2020) 5-26,

[67] Yue, Hongwei, Hongtao Wang, Huazhou Chen, Ken Cai, Yingying Jin, Automatic detection of feather defects using Lie group and fuzzy Fisher criterion for shuttlecock production, *Mechanical Systems and Signal Processing*, 141 (2020) 106690,

[68] Zenggang, Xiong, Tang Zhiwen, Chen Xiaowen, Zhang Xue-min, Zhang Kaibin, Ye Conghuan, Research on image retrieval algorithm based on combination of color and shape features, *Journal of signal processing systems*, 93 (2021) 139-146,

[69] Zhang, Tao, Xinyue He, Yixin Deng, Daniel CW Tsang, Huimin Yuan, Jianbo Shen, Shicheng Zhang, Swine manure valorization for phosphorus and nitrogen recovery by catalytic-thermal hydrolysis and struvite crystallization, *Science of The Total Environment*, 729 (2020) 138999,

[70] Hu, Xin, Heap-Yih Chong, Xiangyu Wang, Sustainability perceptions of off-site manufacturing stakeholders in Australia, *Journal of Cleaner Production*, 227 (2019) 346-354,

[71] Zhang, Bo, Zhongqian Niu, Jiale Wang, Dongfeng Ji, Tianchi Zhou, Yang Liu, Yinian Feng, Yi Hu, Jicong Zhang, Yong Fan, Four - hundred gigahertz broadband multi - branch waveguide coupler, *IET Microwaves, Antennas & Propagation*, 14 (2020) 1175-1179,

[72] Keshtegar, Behrooz, Salim Heddam, Abderrazek Sebbar, Shun-Peng Zhu, Nguyen-Thoi Trung, SVR-RSM: a hybrid heuristic method for modeling monthly pan evaporation, *Environmental Science and Pollution Research*, 26 (2019) 35807-35826,

[73] Seo, Byeongmo, Yeo Beom Yoon, Suwon Song Soolyeon Cho, ANN-based thermal load prediction approach for advanced controls in building energy systems, *ARCC Conference Repository*, 2019.

[74] Halon, Tomasz, Ewa Pelinska-Olko, Malgorzata Szyc, Bartosz Zajaczkowski, Predicting performance of a district heat powered adsorption chiller by means of an artificial neural network, *Energies*, 12 (2019) 3328,

[75] Nguyen, Hoang, Hossein Moayedi, Wan Amizah Wan Jusoh, Abolhasan Sharifi, Proposing a novel predictive technique using M5Rules-PSO model estimating cooling load in energy-efficient building system, *Engineering with Computers*, 36 (2020) 857-866,

[76] Koschwitz, Daniel, Eric Spinnraeker, Jérôme Frisch, Christoph van Treeck, Long-term urban heating load predictions based on optimized retrofit orders: A cross-scenario analysis, *Energy and Buildings*, 208 (2020) 109637,

[77] Roy, Sanjiban Sekhar, Pijush Samui, Ishan Nagtode, Hemant Jain, Vishal Shivaramakrishnan, Behnam Mohammadi-Ivatloo, Forecasting heating and cooling loads of buildings: A comparative performance analysis, *Journal of Ambient Intelligence and Humanized Computing*, 11 (2020) 1253-1264, <https://doi.org/10.1007/s12652-019-01317-y>.

[78] Nilashi, Mehrbakhsh, Mohammad Dalvi-Esfahani, Othman Ibrahim, Karamollah Bagherifard, Abbas Mardani, Norhayati Zakuan, A soft computing method for the prediction of energy performance of residential buildings, *Measurement*, 109 (2017) 268-280,

[79] Pezeshki, Zahra, Sayyed Majid Mazinani, Comparison of artificial neural networks, fuzzy logic and neuro fuzzy for predicting optimization of building thermal consumption: a survey, *Artificial Intelligence Review*, 52 (2019) 495-525,

[80] Naji, Sareh, Shahaboddin Shamshirband, Hossein Basser, Afram Keivani, U Johnson Alengaram, Mohd Zamin Jumaat, Dalibor Petković, Application of adaptive neuro-fuzzy methodology for estimating building energy consumption, *Renewable and Sustainable Energy Reviews*, 53 (2016) 1520-1528,

[81] Chou, Jui-Sheng, Dac-Khuong Bui, Modeling heating and cooling loads by artificial intelligence for

energy-efficient building design, *Energy and Buildings*, 82 (2014) 437-446,

[82] Moayedi, Hossein, Dieu Tien Bui, Anastasios Dounis, Phuong Thao Thi Ngo, A novel application of league championship optimization (LCA): hybridizing fuzzy logic for soil compression coefficient analysis, *Applied sciences*, 10 (2019) 67,

[83] Satrio, Pujo, Teuku Meurah Indra Mahlia, Niccolo Giannetti, Kiyoshi Saito, Optimization of HVAC system energy consumption in a building using artificial neural network and multi-objective genetic algorithm, *Sustainable Energy Technologies and Assessments*, 35 (2019) 48-57,

[84] Nguyen, Hoang, Mohammad Mehrabi, Bahareh Kalantar, Hossein Moayedi, Mu'azu Mohammed Abdullahi, Potential of hybrid evolutionary approaches for assessment of geo-hazard landslide susceptibility mapping, *Geomatics, Natural Hazards and Risk*, 10 (2019) 1667-1693,

[85] Moayedi, Hossein, Hoang Nguyen, Loke Kok Foong, Nonlinear evolutionary swarm intelligence of grasshopper optimization algorithm and gray wolf optimization for weight adjustment of neural network, *Engineering with Computers*, 37 (2021) 1265-1275,

[86] Mirjalili, Seyedali, Andrew Lewis, The whale optimization algorithm, *Advances in engineering software*, 95 (2016) 51-67,

[87] Aziz, Mohamed Abd El, Ahmed A Ewees, Aboul Ella Hassanien, Multi-objective whale optimization algorithm for content-based image retrieval, *Multimedia tools and applications*, 77 (2018) 26135-26172,

[88] Wang, Jianzhou, Pei Du, Tong Niu, Wendong Yang, A novel hybrid system based on a new proposed algorithm—Multi-Objective Whale Optimization Algorithm for wind speed forecasting, *Applied energy*, 208 (2017) 344-360,

[89] Kumawat, Ishwar Ram, Satyasai Jagannath Nanda, Ravi Kumar Maddila, Multi-objective whale optimization, *Tencon 2017-2017 ieee region 10 conference, IEEE, 2017*, pp. 2747-2752.

[90] Roberts, Andrew, Andrew Marsh, ECOTECT: environmental prediction in architectural education, (2001),

[91] Tsanas, Athanasios, Angeliki Xifara, Accurate quantitative estimation of energy performance of residential buildings using statistical machine learning tools, *Energy and buildings*, 49 (2012) 560-567, <https://doi.org/10.1016/j.enbuild.2012.03.003>.

[92] Pessenlehner, Werner, Ardesir Mahdavi, Building morphology, transparency, and energy performance, na, 2003.

[93] Ouarghi, Ramzi, Moncef Krarti, Building Shape Optimization Using Neural Network and Genetic Algorithm Approach, *Ashrae transactions*, 112 (2006),

[94] Schiavon, Stefano, Kwang Ho Lee, Fred Bauman, Tom Webster, Influence of raised floor on zone design cooling load in commercial buildings, *Energy and Buildings*, 42 (2010) 1182-1191,

[95] Huang, Yu, Jian-lei Niu, Tse-ming Chung, Comprehensive analysis on thermal and daylighting performance of glazing and shading designs on office building envelope in cooling-dominant climates, *Applied energy*, 134 (2014) 215-228,

[96] McCulloch, Warren S, Walter Pitts, A logical calculus of the ideas immanent in nervous activity, *Bulletin of mathematical biology*, 52 (1990) 99-115,

[97] Moayedi, Hossein, Abbas Rezaei, An Artificial Neural Network Approach for Under Reamed Piles Subjected to Uplift Forces in Dry Sand, *Neural Computing and Applications*, 31 (2019), 10.1007/s00521-017-2990-z.

[98] Moayedi, Hossein, Sajad Hayati, Applicability of a CPT-based neural network solution in predicting load-settlement responses of bored pile, *International Journal of Geomechanics*, 18 (2018) 06018009,

[99] Whitley, Darrell, A genetic algorithm tutorial, *Statistics and Computing*, 4 (1994) 65-85, 10.1007/BF00175354.

[100] Moayedi, Hossein, Mehdi Raftari, Abolhasan Sharifi, Wan Amizah Wan Jusoh, Ahmad Safuan A. Rashid, Optimization of ANFIS with GA and PSO estimating  $\alpha$  ratio in driven piles, *Engineering with Computers*, 36 (2019) 227-238,

[101] Atashpaz-Gargari, Esmaeil, Caro Lucas, Imperialist competitive algorithm: An algorithm for optimization inspired by imperialistic competition, *2007 IEEE Congress on Evolutionary Computation*, (2007) 4661-4667,

[102] Hof, Patrick R, Estel Van der Gucht, Structure of the cerebral cortex of the humpback whale, *Megaptera novaeangliae* (Cetacea, Mysticeti, Balaenopteridae), *The Anatomical Record: Advances in Integrative Anatomy and Evolutionary Biology: Advances in Integrative Anatomy and Evolutionary Biology*, 290 (2007) 1-31,

[103] Watkins, William A, William E Schevill, Aerial observation of feeding behavior in four baleen whales: *Eubalaena glacialis*, *Balaenoptera borealis*, *Megaptera novaeangliae*, and *Balaenoptera physalus*, *Journal of Mammalogy*, 60 (1979) 155-163,

[104] Goldbogen, Jeremy A, Ari S Friedlaender, John Calambokidis, Megan F McKenna, Malene Simon, Douglas P Nowacek, Integrative approaches to the study of baleen whale diving behavior, feeding performance, and foraging ecology, *BioScience*, 63 (2013) 90-100,

[105] Seyedashraf, Omid, Mohammad Mehrabi, Ali Akbar Akhtari, Novel approach for dam break flow modeling using computational intelligence, *Journal of Hydrology*, 559 (2018) 1028-1038,

[106] Mosallanezhad, Mansour, Hossein Moayedi, Developing hybrid artificial neural network model for predicting uplift resistance of screw piles, *Arabian Journal of Geosciences*, 10 (2017) 1-10,

[107] Deng, Hengfang, David Fannon, Matthew J Eckelman, Predictive modeling for US commercial building energy use: A comparison of existing statistical and machine learning algorithms using CBECS microdata, *Energy and Buildings*, 163 (2018) 34-43,